Supplemental information

1. Additional VPRM methods:

All flux tower NEE and meteorological data was downloaded from the AmeriFlux (https://ameriflux.lbl.gov/) and National Ecological Observatory Network (NEON; https://www.neonscience.org/) websites and u-star filtered using site-specific thresholds (Barr et al., 2013). Including historical towers that are no longer operational allows us to include many more spatial locations in the optimization than if we only relied on towers which are currently running. In fact, 46 of the 69 flux towers used in this study were not included in either Mahadevan et al. (2008) or Hilton et al., (2013, 2014). However, the distribution of flux tower site-years in our database is heavily tilted towards the north of the domain, with grassland and wetland sites under-represented, particularly in the developed-open category (i.e. suburban lawns, parks and gardens) and the coastal Carolinas. Also, despite the large number of forest sites in the database (42 out of 69), there are few sites in the Appalachian deciduous forests and the northern mixed forests in Canada. Therefore, in order to the spatial representativeness of sites in the database, data from northern sites with long records were sub-sampled to emphasize more recent years and some sites in coincident locations were removed (e.g. US-NE1), but even after this procedure, 70% of site-years in the database are still north of 40°N.

Gridded land cover maps are taken from the National Land Cover Database 2016 (NLCD2016; Yang et al., 2018) in the USA, with corn and other crop areas determined from the Cropland Data Layer (Boryan et al., 2011) specifically for 2017. In Canada, the Agriculture and Agri-Food Canada Annual Crop Inventory 2017 (Agriculture and Agri-Food Canada, 2016); which includes non-crop land cover types as well) was used. All high-resolution (i.e 30 m) land-cover products were aggregated up to 0.02 degree to determine fractional coverage across pixels in our domain.

Enhanced Vegetation Index (EVI) and Land Surface Water Index (LSWI) are extracted from the MODIS Aqua and Terra products MOD13A2/MYD13A2 and MOD09A1/MYD09A1 at 1 km and 500 m resolution respectively, and then aggregated up to 0.02 degree for the gridded runs. A daily interpolation is performed across EVI and LSWI values from 8 and 16-day composites respectively using the actual dates of the satellite overpass within the composite period for each pixel. Using the satellite overpass dates in the interpolation has been shown to help improve the simulation of phenology with remotely-sensed vegetation indices, particularly in croplands with short growing seasons (Guindin-Garcia et al., 2012; Lokupitiya et al., 2009). However, the actual gap between successive overpasses can be as short as one or as long as 24 days (with an average interval of 8 days for EVI and 4 days for LSWI). For the parameter optimization, 500 m EVI from the MOD13Q1/MYD13Q1 products and 500m LSWI from MOD09A1/MYD09A1 are extracted at each flux tower location using the R package MODISTools (https://cran.r-project.org/web/packages/MODISTools/index.html). For the EVI and LSWI values at the flux towers, the dates for interpolation were assumed as the middle of each composite period in the absence of satellite overpass information.

Gridded air temperature and shortwave radiation data are taken from the High Resolution Rapid Refresh (HRRR; Benjamin et al., 2016) model, which is at 3-km resolution and then downscaled to 0.02 degree. The high spatial resolution of the HRRR product relative to other meteorological products (like NLDAS,

Xia et al., 2012, or the WRF runs for this domain) helps to simulate temperature gradients in urban and mountainous areas better than with coarser-resolution products (Figure S1.1). Many radiation products are known to have a clear-sky bias (i.e. they under-represent cloudy conditions; Slater, 2016), including the HRRR radiation product used here, although the HRRR biases are less than those with WRF (as seen in a comparison to flux tower and NEON tower observations and other models in our domain, Figure S1.2). Although biases in the gridded meteorological data can bias flux estimates, we considered the magnitude of these biases to be small relative to other sources of error, and therefore, did not bias-correct the gridded temperature or radiation data. Site-specific weather variables are also used in the parameter optimization, rather than modeled met data at each flux tower site, which could potentially compensate for biases in the meteorological products.

Figure S1.1: Comparison of gridded temperature data from HRRR, NLDAS and WRF to surface observations at nine NEON and AmeriFlux towers within our domain from Nov. 1, 2016 to Oct. 31, 2017. Daytime and night-time mean biases are shown in the left and center plots, and 24-hour root mean squared errors (RMSE) in the right plot. HRRR data is at 3 km spatial resolution, NLDAS at 1/8th degree (~12 km), and WRF at 9 km (with 1 km and 3 km nests around Washington DC/ Baltimore.)
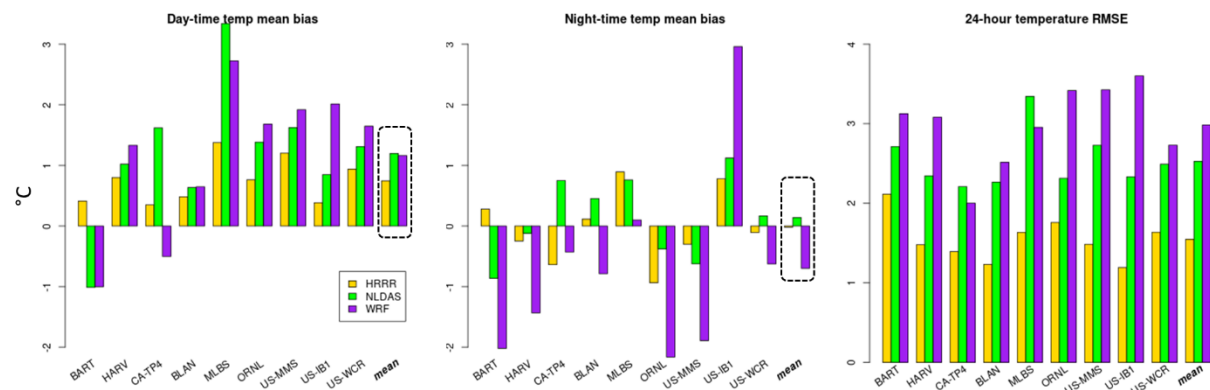
Figure S1.2: Comparison of gridded shortwave radiation data from HRRR, NLDAS and WRF to surface observations at NEON and AmeriFlux towers. Daytime mean biases and the hourly root mean squared errors (RMSE) are shown for each tower, plus the average across towers. Also shown is the distribution of hourly radiation across all towers within four bins (<=150 W/m^2, 150 to 300 W/m^2, 300 to 600 W/m^2 and 600 to 1000 W/m^2) for each model and the observations.
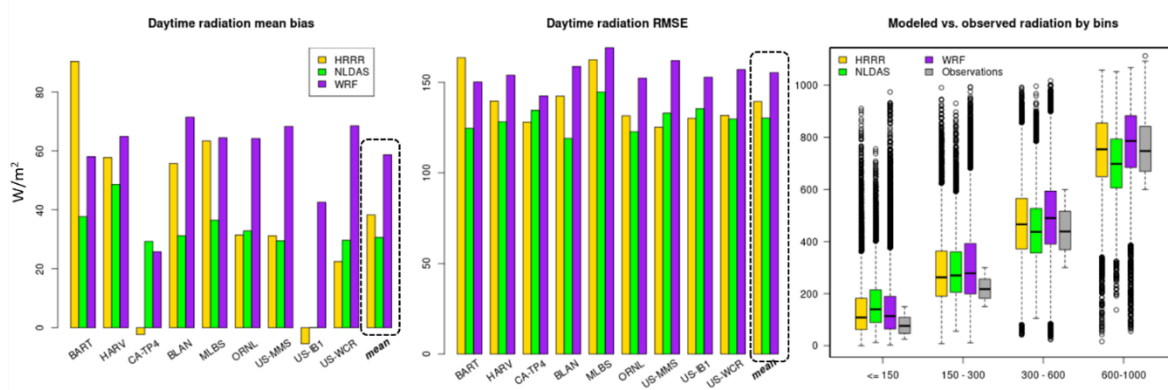
2. Determination of afternoon hours in atmospheric CO_2 observations

In this study, "afternoon" hours are defined as hours when the middle falls five hours after sunrise and just before sunset, thus increasing the number of observations during the height of the growing season relative to studies that use a fixed interval, e.g. 12 pm – 4 pm local time. For example, at DNH (Durham, NH) in the north of the domain, sunrise and sunset on July 1, 2017 are at 5:12 am and 8:35 pm EDT, and thus we would use eleven hourly observations from 10 am - 9 pm EDT on this day. This definition of afternoon hours relative to sunrise and sunset time was determined by examining vertical gradients in measurements across inlet heights (on towers with multiple inlets) to identify when well-mixed conditions are most likely to occur. As seen in Figure 2d in the main text, the gradient across towers during afternoon hours during the growing season (July) is lower compared to at other times of the day.

3. Customized WRF and STILT runs to generate footprints

Following Lopez-Coto et al. (2020), WRF is configured with three nested domains (9 km, 3 km, and 1 km), with the innermost domain covering the urban area of interest, and 60 vertical levels with monotonically increasing thickness from the surface (34 levels below 3 km) for better boundary layer representation. WRF model runs are configured with the RRTMG radiation scheme (Mlawer et al., 1997), Thompson microphysics scheme (Thompson et al., 2004, 2008), Noah land surface model (Chen & Dudhia, 2001), the Kain-Fritsch cumulus scheme (for the 9 km domain only; Kain, 2004), the 1.5- order closure scheme MYNN (Nakanishi & Niino, 2004, 2006) with the eddy mass-flux option (Olson et al., 2019) and the land-use classification from NLCD 2011 (Yang et al., 2018b) which includes four urban categories, from developed open space to developed high intensity. They are also driven by initial and boundary conditions from the North America Regional Reanalysis (NARR) three hourly data (Mesinger et al., 2006).

In STILT, 960 particles were released at each observation location and time period, and then tracked back for 120 hours (at which point the influence of fluxes inside the domain is assumed minimal). Particle influences were summed within each pixel and hour to determine a spatially and temporally-varying footprint at a 0.1° hourly resolution. A far-field footprint correction (based on work originally done by Fasoli et al., 2018, but modified at NIST) was also implemented to smooth out the discrete nature of the atmospheric influence far away from the towers caused by the limited number of particles released.

References from the Supporting Information

Agriculture and Agri-Food Canada. (2016). Annual Crop Inventory. *2017*. Retrieved from
        https://open.canada.ca/data/en/dataset/ba2645d5-4458-414d-b196-6303ac06c1c9
Baker, I., Denning, S., & Stöckli, R. (2010). North American gross primary productivity: regional characterization and
        interannual variability. *Tellus B: Chemical and Physical Meteorology*, *62*(5), 533–549.
        https://doi.org/10.1111/j.1600-0889.2010.00492.x
Barr, A. G., Richardson, A. D., Hollinger, D. Y., Papale, D., Arain, M. A., Black, T. A., et al. (2013). Use of change-point
        detection for friction–velocity threshold evaluation in eddy-covariance studies. *Agricultural and Forest
        Meteorology*, *171–172*, 31–45. https://doi.org/10.1016/j.agrformet.2012.11.023

Benjamin, S. G., Weygandt, S. S., Brown, J. M., Hu, M., Alexander, C. R., Smirnova, T. G., et al. (2016). A North American Hourly Assimilation and Model Forecast Cycle: The Rapid Refresh. *Monthly Weather Review*, *144*(4), 1669–1694. https://doi.org/10.1175/MWR-D-15-0242.1

Boryan, C., Yang, Z., Mueller, R., & Craig, M. (2011). Monitoring US agriculture: the US Department of Agriculture, National Agricultural Statistics Service, Cropland Data Layer Program. *Geocarto International*, *26*(5), 341–358. https://doi.org/10.1080/10106049.2011.562309

Chen, F., & Dudhia, J. (2001). Coupling an Advanced Land Surface–Hydrology Model with the Penn State–NCAR MM5 Modeling System. Part II: Preliminary Model Validation. https://doi.org/10.1175/1520-0493(2001)129<0587:CAALSH>2.0.CO;2

Fasoli, B., Lin, J. C., Bowling, D. R., Mitchell, L., & Mendoza, D. (2018). Simulating atmospheric tracer concentrations for spatially distributed receptors: updates to the Stochastic Time-Inverted Lagrangian Transport model's R interface (STILT-R version 2). *Geoscientific Model Development*, *11*(7), 2813–2824. https://doi.org/10.5194/gmd-11-2813-2018

Guindin-Garcia, N., Gitelson, A. A., Arkebauer, T. J., Shanahan, J., & Weiss, A. (2012). An evaluation of MODIS 8- and 16-day composite products for monitoring maize green leaf area index. *Agricultural and Forest Meteorology*, *161*, 15–25. https://doi.org/10.1016/j.agrformet.2012.03.012

Haynes, K. D., Baker, I. T., Denning, A. S., Stöckli, R., Schaefer, K., Lokupitiya, E. Y., & Haynes, J. M. (2019). Representing Grasslands Using Dynamic Prognostic Phenology Based on Biological Growth Stages: 1. Implementation in the Simple Biosphere Model (SiB4). *Journal of Advances in Modeling Earth Systems*, *11*(12), 4423–4439. https://doi.org/10.1029/2018MS001540

Hilton, T. W., Davis, K. J., Keller, K., & Urban, N. M. (2013). Improving North American terrestrial CO_2 flux diagnosis using spatial structure in land surface model residuals. *Biogeosciences*, *10*(7), 4607–4625. https://doi.org/10.5194/bg-10-4607-2013

Hilton, T. W., Davis, K. J., & Keller, K. (2014). Evaluating terrestrial CO_2 flux diagnoses and uncertainties from a simple land surface model and its residuals. *Biogeosciences*, *11*(2), 217–235. https://doi.org/10.5194/bg-11-217-2014

Kain, J. S. (2004). The Kain–Fritsch Convective Parameterization: An Update. *Journal of Applied Meteorology and Climatology*, *43*(1), 170–181. https://doi.org/10.1175/1520-0450(2004)043<0170:TKCPAU>2.0.CO;2

Lawrence, P. J., & Chase, T. N. (2007). Representing a new MODIS consistent land surface in the Community Land Model (CLM 3.0). *Journal of Geophysical Research: Biogeosciences*, *112*(G1). https://doi.org/10.1029/2006JG000168

Lokupitiya, E., Denning, S., Paustian, K., Baker, I., Schaefer, K., Verma, S., et al. (2009). Incorporation of crop phenology in Simple Biosphere Model (SiBcrop) to improve land-atmosphere carbon exchanges from croplands. *Biogeosciences*, *6*(6), 969–986. https://doi.org/10.5194/bg-6-969-2009

Lopez-Coto, I., Hicks, M., Karion, A., Sakai, R. K., Demoz, B., Prasad, K., & Whetstone, J. (2020). Assessment of Planetary Boundary Layer Parameterizations and Urban Heat Island Comparison: Impacts and Implications for Tracer Transport. *Journal of Applied Meteorology and Climatology*, *59*(10), 1637–1653. https://doi.org/10.1175/JAMC-D-19-0168.1

Mahadevan, P., Wofsy, S. C., Matross, D. M., Xiao, X., Dunn, A. L., Lin, J. C., et al. (2008). A satellite-based biosphere parameterization for net ecosystem CO2 exchange: Vegetation Photosynthesis and Respiration Model (VPRM). *Global Biogeochemical Cycles*, *22*(2). https://doi.org/10.1029/2006GB002735

Mesinger, F., DiMego, G., Kalnay, E., Mitchell, K., Shafran, P. C., Ebisuzaki, W., et al. (2006). North American Regional Reanalysis. *Bulletin of the American Meteorological Society*, *87*(3), 343–360. https://doi.org/10.1175/BAMS-87-3-343

Mlawer, E. J., Taubman, S. J., Brown, P. D., Iacono, M. J., & Clough, S. A. (1997). Radiative transfer for inhomogeneous atmospheres: RRTM, a validated correlated-k model for the longwave. *Journal of Geophysical Research: Atmospheres*, *102*(D14), 16663–16682. https://doi.org/10.1029/97JD00237

Nakanishi, M., & Niino, H. (2004). An Improved Mellor–Yamada Level-3 Model with Condensation Physics: Its Design and Verification. *Boundary-Layer Meteorology*, *112*(1), 1–31. https://doi.org/10.1023/B:BOUN.0000020164.04146.98

Nakanishi, M., & Niino, H. (2006). An Improved Mellor–Yamada Level-3 Model: Its Numerical Stability and Application to a Regional Prediction of Advection Fog. *Boundary-Layer Meteorology*, *119*(2), 397–407. https://doi.org/10.1007/s10546-005-9030-8

Olson, J. B., Kenyon, J. S., Angevine, W. A., Brown, J. M., Pagowski, M., & Suselj, K. (2019). A Description of the MYNN-EDMF Scheme and the Coupling to Other Components in WRF–ARW. https://doi.org/10.25923/N9WM-BE49

Slater, A. G. (2016). Surface Solar Radiation in North America: A Comparison of Observations, Reanalyses, Satellite, and Derived Products. *Journal of Hydrometeorology*, *17*(1), 401–420. https://doi.org/10.1175/JHM-D-15-0087.1

Thompson, G., Rasmussen, R. M., & Manning, K. (2004). Explicit Forecasts of Winter Precipitation Using an Improved Bulk Microphysics Scheme. Part I: Description and Sensitivity Analysis. *Monthly Weather Review*, *132*(2), 519–542. https://doi.org/10.1175/1520-0493(2004)132<0519:EFOWPU>2.0.CO;2

Thompson, G., Field, P. R., Rasmussen, R. M., & Hall, W. D. (2008). Explicit Forecasts of Winter Precipitation Using an Improved Bulk Microphysics Scheme. Part II: Implementation of a New Snow Parameterization. *Monthly Weather Review*, *136*(12), 5095–5115. https://doi.org/10.1175/2008MWR2387.1

Xia, Y., Mitchell, K., Ek, M., Sheffield, J., Cosgrove, B., Wood, E., et al. (2012). Continental-scale water and energy flux analysis and validation for the North American Land Data Assimilation System project phase 2 (NLDAS-2): 1. Intercomparison and application of model products. *Journal of Geophysical Research: Atmospheres*, *117*(D3). https://doi.org/10.1029/2011JD016048

Yang, L., Jin, S., Danielson, P., Homer, C., Gass, L., Bender, S. M., et al. (2018a). A new generation of the United States National Land Cover Database: Requirements, research priorities, design, and implementation strategies. *ISPRS Journal of Photogrammetry and Remote Sensing*, *146*, 108–123. https://doi.org/10.1016/j.isprsjprs.2018.09.006

Yang, L., Jin, S., Danielson, P., Homer, C., Gass, L., Bender, S. M., et al. (2018b). A new generation of the United States National Land Cover Database: Requirements, research priorities, design, and implementation strategies. *ISPRS Journal of Photogrammetry and Remote Sensing*, *146*, 108–123. https://doi.org/10.1016/j.isprsjprs.2018.09.006

Zhou, Y., Williams, C. A., Lauvaux, T., Davis, K. J., Feng, S., Baker, I., et al. (2020). A Multiyear Gridded Data Ensemble of Surface Biogenic Carbon Fluxes for North America: Evaluation and Analysis of Results. *Journal of Geophysical Research: Biogeosciences*, *125*(2), e2019JG005314. https://doi.org/10.1029/2019JG005314

Table S1: Characteristics of biospheric models included in the inter-comparison.

	VPRM (Mahadevan et al, 2008; this study)	CASA (Zhou et al, 2020)	SiB4v2 (Haynes et al, 2019)
Spatial resolution	0.02 degree	5km	0.5 degree
Temporal resolution	hourly	monthly, downscaled to 3-hourly with temperature & radiation	hourly
Phenology	diagnostic (based on 8-day MODIS EVI/LSWI from overlapping 16-day composites)	diagnostic (based on monthly MODIS fPAR)	prognostic, climate-driven, daily temporal resolution
Photosynthesis model	light-use efficiency with downscaling for temperature & water stress	light-use efficiency with downscaling for temperature & water stress	enzyme-kinetic (operates at sub-hourly timescale)
Respiration model	**original model**: linear function of temperature for each PFT, **new respiration model**: function of quadratic temperature, water stress and interactions with temperature, and EVI	3 live carbon pools (leaves, stem, roots), 3 litter pools, 5 soil and 2 coarse woody debris pools. Autotrophic respiration = 0.5*GPP; heterotrophic respiration = sources from dead carbon pools as a function of pool-specific decay rate constants, effects of soil moisture, temperature (with a Q10 relationship) and microbial decomposition efficiency	5 live carbon pools (leaf, wood, products, fine and coarse roots) and 6 dead carbon pools (2 surface litter, coarse woody debris and 3 soil); respiration fluxes determined using current photosynthetic uptake and decay rate constants with environmental limitations for all pools
Parameter selection	optimized using NEE observations from flux towers in eastern US & Canada operating since 2001. **original model**: optimized with 24 hours of hourly flux tower NEE observations, **new respiration model**: respiration parameters optimized with night-time average flux tower NEE observations, GPP parameters optimized with hourly day-time GPP "observations" (i.e. NEE - predicted respiration)	GPP parameters calibrated with flux tower partitioned GPP observations from towers across North America; ensemble approach where individual members vary light-use efficiency, T_{opt} and Q10; ensemble mean across 27 members of L2 product used here	From literature, previous versions of SiB
Land cover map	USA: NLCD2016 for all categories, except crops (https://www.mrlc.gov/data/nlcd-2016-land-cover-conus); crops from Cropland Data Layer (https://www.nass.usda.gov/Research_and_Science/Cropland/Release/). Canada: Canadian Annual Crop Inventory 2017 for all categories (https://open.canada.ca/data/en/dataset/ba2645d5-4458-414d-b196-6303ac06c1c9).	MOD12Q1 Global Land Cover, modified with National Forest Type and North American Forest Dynamics products; tree and grass cover from MOD44B Vegetation Continuous Fields	MOD12Q1 Global Land Cover, modified for CLM 3.0 as in Lawrence and Chase (2007)
Land-cover within pixel	weighted fractional coverage	dominant land-use	weighted fractional coverage
Plant functional types	Deciduous broadleaf forests, Evergreen needleleaf/mixed forests (>40N), Evergreen needleleaf/ mixed forests (<40N), Grass/pasture/dev-open, Shrub/savannah, wetlands, corn, other crops	From MODIS IGBP: evergreen needleleaf forests, deciduous broadleaf forests, mixed forests, closed and open shrublands, woody (and non-woody) savannahs, grasslands, croplands, urban and built-up, cropland/natural vegetation mosaic	In this domain: evergreen needleleaf forest, deciduous broadleaf forest, shrubs, C3 grasslands, C4 grasslands, maize, soybean, wheat, generic C3 crops
Crops	corn vs. other crops (separate parameters & land-cover)	single crop type	separate parameters for corn, wheat, soybean and generic C3 and C4 crops; crop-specific prognostic phenology determined by growing-degree-days
Urban	Low, medium and high intensity developed land classified as urban; heterotrophic respiration (i.e. half of total respiration) reduced by fraction of impervious surface coverage (Hardiman et al, 2017); developed-open included with grasslands	zero flux when dominant land-cover	not separately simulated (no urban PFT)
Meteorological variables	air temperature and shortwave radiation	air temperature, total precipitation, shortwave and longwave radiation	air temperature, precipitation, shortwave and longwave radiation, surface pressure, wind speed, specific humidity
Meteorological model	HRRR (3km resolution)	NARR (32 km resolution; 3-hourly) for 5 km North American runs and for temporal downscaling; PRISM for precipitation and air temperature in 500 m runs; NLDAS-2 for radiation in 500 m runs	MERRA, regridded to 0.5° resolution; precipitation scaled to GPCP (as in Baker et al, 2010)

Table S2: flux towers used in the VPRM parameter optimization, along with ancillary information. All data was downloaded from the AmeriFlux (ameriflux.lbl.gov) and NEON (neonscience.org) websites, with NEON towers indicated in the description.

	Description	State/ Province	Latitude	Longitude	Vegetation Description (IGBP)	PFT, this study	Years included in optimization	Included in Hilton et al or Mahadevan et al?	Dataset reference
CA-Gro	Groundhog River, Boreal Mixedwood Forest	Ontario	48.217	-82.156	Mixed Forests	Evergreen/mixed forests > 40N	2003-2014	Hilton	McCaughey (2003-)
CA-TP1	Turkey Point 2002 Plantation White Pine	Ontario	42.661	-80.560	Evergreen Needleleaf Forests	Evergreen/mixed forests > 40N	2005-2014		Arain (2003-)
CA-TP3	Turkey Point 1974 Plantation White Pine	Ontario	42.707	-80.348	Evergreen Needleleaf Forests	Evergreen/mixed forests > 40N	2012-2016		Arain (2003-)
CA-TPD	Turkey Point Mature Deciduous	Ontario	42.635	-80.558	Deciduous Broadleaf Forests	Deciduous broadleaf forests	2012-2016		Arain (2012-)
TALL	Talladega National Forest (NEON)	Alabama	32.951	-87.393	Mixed Forests	Evergreen/mixed forests < 40N	2018-2019		Sturtevant et al (2017-)
US-ARC	ARM Southern Great Plains control site	Oklahoma	35.546	-98.040	Grasslands	Grass/pasture	2005-2006		Torn et al (2005-2006)
US-ARM	ARM Southern Great Plains	Oklahoma	36.606	-97.489	Croplands	Crops, other	2003-2004; 2006-2012	Hilton	Biraud et al (2002-)
US-Bar	Bartlett Experimental Forest (AmeriFlux/NEON)	New Hampshire	44.065	-71.288	Deciduous Broadleaf Forests	Deciduous broadleaf forests	2004-2016; 2018-2019		Richardson & Hollinger (2004-)
US-Bo1	Bondville	Illinois	40.006	-88.290	Croplands	Corn/ Crops, other	Corn: 2001, 2005, 2007 Soybean: 2004, 2006	Mahadevan, Hilton	Meyers (1996-)
US-Bo2	Bondville (companion site)	Illinois	40.009	-88.290	Croplands	Corn	2006	HIlton	Bernacchi (2004-2008)
US-Br1	Brooks Field Site 10- Ames	Iowa	41.975	-93.691	Croplands	Corn/ Crops, other	Corn: 2005, 2007, 2011 Soybean: 2006, 2010		Prueger & Parkin (2001)
US-Br3	Brooks Field Site 11- Ames	Iowa	41.975	-93.694	Croplands	Corn/ Crops, other	Corn: 2006, 2010 Soybean: 2005		Prueger & Parkin (2001)
US-CaV	Canaan Valley	West Virginia	39.063	-79.421	Grasslands	Grass/pasture	2004, 2008-2009	Hilton	Meyers (2004-)
US-Ced	Cedar Bridge	New Jersey	39.838	-74.379	Closed Shrublands	Shrubs	2006-2014		Clark (2005-)
US-ChR	Chestnut Ridge	Tennessee	35.931	-84.332	Deciduous Broadleaf Forests	Deciduous broadleaf forests	2006-2009		Meyers (2005-)
US-CRT	Curtice Walter-Berger cropland	Ohio	41.629	-83.347	Croplands	Crops, other	2011, 2012, 2013		Chen & Chu (2011-2013)
US-Dix	Fort Dix	New Jersey	39.971	-74.435	Mixed Forests	Evergreen/mixed forests < 40N	2005-2008		Clark (2005-2008)

US-Dk1	Duke Forest-open field	North Carolina	35.971	-79.093	Grasslands	Grass/pasture	2001-2005	Mahadevan, Hilton	Oishi et al (2001-2008)
US-Dk2	Duke Forest-hardwoods	North Carolina	35.974	-79.100	Deciduous Broadleaf Forests	Deciduous broadleaf forests	2001	Mahadevan, Hilton	Oishi et al (2001-2008)
US-Dk3	Duke Forest - loblolly pine	North Carolina	35.978	-79.094	Evergreen Needleleaf Forests	Evergreen/mixed forests < 40N	2001-2006	Hilton	Oishi et al (2001-2008)
US-FR3	Freeman Ranch - Woodland	Texas	29.940	-97.990	Closed Shrublands	Shrubs	2009-2012		Heilman (2004-)
US-GMF	Great Mountain Forest	Connecticut	41.967	-73.233	Mixed Forests	Evergreen/mixed forests > 40N	2001-2003		Lee (1999-2004)
US-Goo	Goodwin Creek	Mississippi	34.255	-89.874	Grasslands	Grass/pasture	2002, 2004-2006	Hilton	Meyers (2002-2006)
US-Ha1	Harvard Forest EMS Tower (AmeriFlux/NEON)	Massachusetts	42.538	-72.172	Deciduous Broadleaf Forests	Deciduous broadleaf forests	2001-2012, 2015, 2018-2019	Mahadevan, Hilton	Munger (1991-)
US-Ha2	Harvard Forest Hemlock Site	Massachusetts	42.539	-72.178	Evergreen Needleleaf Forests	Evergreen/mixed forests > 40N	2006-2008, 2012-2013	Hilton	Hadley & Munger (2004-)
US-Ho1	Howland Forest (main tower)	Maine	45.204	-68.740	Evergreen Needleleaf Forests	Evergreen/mixed forests > 40N	2010-2016	Mahadevan, Hilton	Hollinger (1996-)
US-Ho2	Howland Forest (west tower)	Maine	45.209	-68.747	Evergreen Needleleaf Forests	Evergreen/mixed forests > 40N	2001-2009	Hilton	Hollinger (1999-)
US-Ho3	Howland Forest (harvest site)	Maine	45.207	-68.725	Evergreen Needleleaf Forests	Evergreen/mixed forests > 40N	2004-2005		Hollinger (2000-)
US-IB1	Fermi National Accelerator Laboratory-Batavia (Agricultural site)	Illinois	41.859	-88.223	Croplands	Corn/ Crops, other	Corn: 2006, 2008, 2010, 2012, 2013, 2016 Soybean: 2005, 2007, 2009, 2011, 2014, 2015		Matamala (2005-)
US-IB2	Fermi National Accelerator Laboratory-Batavia (Prairie site)	Illinois	41.841	-88.241	Grasslands	Grass/pasture	2009-2011, 2015-2016		Matamala (2004-)
US-KS2	Kennedy Space Center (scrub oak)	Florida	28.609	-80.672	Closed Shrublands	Shrubs	2003-2006	Hilton	Drake & Hinkle (2000-2007)
US-KUT	KUOM Turfgrass Field	Minnesota	44.995	-93.186	Grasslands	Grass/pasture	2006-2009		McFadden (2005-2009)
US-Los	Lost Creek	Wisconsin	46.083	-89.979	Permanent Wetlands	Wetlands	2014-2016	Mahadevan, Hilton	Desai (2001-)
US-MMS	Morgan Monroe State Forest	Indiana	39.323	-86.413	Deciduous Broadleaf Forests	Deciduous broadleaf forests	2012-2016	Mahadevan, Hilton	Novick & Phillips (1999-)
US-MOz	Missouri Ozark Site	Missouri	38.744	-92.200	Deciduous Broadleaf Forests	Deciduous broadleaf forests	2013-2016	Hilton	Wood & Gu (2004-)
US-NC1	NC_Clearcut	North Carolina	35.811	-76.712	Evergreen Needleleaf Forests	Evergreen/mixed forests < 40N	2005-2009		Noormets (2005-2013)

US-NC2	NC_Loblolly Plantation	North Carolina	35.803	-76.669	Evergreen Needleleaf Forests	Evergreen/mixed forests < 40N	2012-2016, 2018		Noormets (2005-)
US-NC3	NC_Clearcut#3	North Carolina	35.799	-76.656	Evergreen Needleleaf Forests	Evergreen/mixed forests < 40N	2015-2016, 2018		Noormets (2013-)
US-NE2	Mead - irrigated maize/ soybean rotation	Nebraska	41.165	-96.470	Croplands	Corn/ Crops, other	Corn: 2009-2012 Soybean: 2002, 2004, 2006, 2008	Mahadevan, Hilton	Suyker (2001-)
US-NE3	Mead - rainfed maize/ soybean rotation	Nebraska	41.180	-96.440	Croplands	Corn/ Crops, other	Corn: 2009, 2011 Soybean: 2008, 2010, 2012	Hilton	Suyker (2001-)
US-Oho	Oak Openings	Ohio	41.555	-83.844	Deciduous Broadleaf Forests	Deciduous broadleaf forests	2005-2007, 2009-2010, 2012		Chen et al (2004-2013)
US-ORv	Olentangy River Wetland Research Park	Ohio	40.020	-83.018	Permanent Wetlands	Wetlands	2011		Bohrer (2011-2016)
US-OWC	Old Woman Creek	Ohio	41.380	-82.513	Permanent Wetlands	Wetlands	2015-2016		Bohrer (2015-2016)
US-PFa	Park Falls/WLEF	Wisconsin	45.946	-90.272	Mixed Forests	Evergreen/mixed forests > 40N	2001-2008	Mahadevan, Hilton	Desai (1996-)
US-Ro1	Rosemount- G21	Minnesota	44.714	-93.090	Croplands	Corn/ Crops, other	Corn: 2005, 2007, 2009, 2011, 2013, 2015 Soybean: 2004, 2006, 2008, 2010, 2012, 2014, 2016		Baker et al (2003-2017)
US-Ro2	Rosemount- C7	Minnesota	44.729	-93.089	Croplands	Crops, other	2016		Baker & Griffis (2003-2017)
US-Ro3	Rosemount- G19	Minnesota	44.722	-93.089	Croplands	Corn/ Crops, other	Corn: 2005, 2007 Soybean: 2004, 2006		Baker & Griffis (2003-2010)
US-Ro4	Rosemount Prairie	Minnesota	44.678	-93.072	Grasslands	Grass/pasture	2015-2016		Baker & Griffis (2014-)
US-Slt	Silas Little	New Jersey	39.914	-74.596	Deciduous Broadleaf Forests	Deciduous broadleaf forests	2010-2014		Clark (2004-)
US-Syv	Sylvania Wilderness Area	Michigan	46.242	-89.348	Mixed Forests	Evergreen/mixed forests > 40N	2001-2002, 2004-2007, 2012-2016	Hilton	Desai (2001-)
US-UMB	Univ. of Mich. Biological Station	Michigan	45.560	-84.714	Deciduous Broadleaf Forests	Deciduous broadleaf forests	2013-2016	Mahadevan, Hilton	Gough et al (1999-)
US-UMd	Univ. of Mich. Biological Station, Disturbance	Michigan	45.563	-84.698	Deciduous Broadleaf Forests	Deciduous broadleaf forests	2016, 2018		Gough et al (2007-)
US-WBW	Walker Branch Watershed	Tennessee	35.959	-84.287	Deciduous Broadleaf Forests	Deciduous broadleaf forests	2004, 2005, 2007		Meyers (1995-1999)
US-WCr	Willow Creek	Wisconsin	45.806	-90.080	Deciduous Broadleaf Forests	Deciduous broadleaf forests	2013-2016	Mahadevan, Hilton	Desai (1999-)

US-Wi1	Intermediate hardwood	Wisconsin	46.731	-91.233	Deciduous Broadleaf Forests	Deciduous broadleaf forests	2003		Chen (2003-2003)
US-Wi4	Mature red pine	Wisconsin	46.739	-91.166	Evergreen Needleleaf Forests	Evergreen/mixed forests > 40N	2005		Chen (2002-2005)
US-Wi5	Mixed young jack pine	Wisconsin	46.653	-91.086	Evergreen Needleleaf Forests	Evergreen/mixed forests > 40N	2004		Chen (2004-2004)
US-Wi7	Red pine clearcut	Wisconsin	46.649	-91.069	Open Shrublands	Shrubs	2005		Chen (2005-2005)
US-Wi8	Young hardwood clearcut	Wisconsin	46.722	-91.252	Deciduous Broadleaf Forests	Deciduous broadleaf forests	2002		Chen (2002-2002)
US-Wi9	Young Jack pine	Wisconsin	46.619	-91.081	Evergreen Needleleaf Forests	Evergreen/mixed forests > 40N	2005		Chen (2004-2005)
US-WPT	Winous Point North Marsh	Ohio	41.465	-82.996	Permanent Wetlands	Wetlands	2011-2013		Chen & Chu (2011-2013)
US-xDL	Dead Lake (NEON)	Alabama	32.542	-87.804	Mixed Forests	Evergreen/mixed forests < 40N	2018		Sturtevant et al (2017-)
US-xGR	Great Smoky Mountains National Park (NEON)	Tennessee	35.689	-83.502	Deciduous Broadleaf Forests	Deciduous broadleaf forests	2019		Sturtevant et al (2017-)
US-xSC	Smithsonian Conservation Biology Unit (NEON)	Virginia	38.893	-78.140	Deciduous Broadleaf Forests	Deciduous broadleaf forests	2018-2019		Sturtevant et al (2016-)
US-xSE	Smithsonian Environmental Research Center (NEON)	Maryland	39.890	-76.560	Deciduous Broadleaf Forests	Deciduous broadleaf forests	2018, 2019		Sturtevant et al (2016-)
US-xST	Steigerwaldt Land Services (NEON)	Wisconsin	45.509	-89.586	Deciduous Broadleaf Forests	Deciduous broadleaf forests	2018-2019		Sturtevant et al (2017-)
US-xTR	Treehaven (NEON)	Wisconsin	45.494	-89.586	Deciduous Broadleaf Forests	Deciduous broadleaf forests	2018-2019		Sturtevant et al (2017-)
US-xUK	University of Kansas Field Station (NEON)	Kansas	39.040	-95.192	Mixed Forests	Evergreen/mixed forests < 40N	2018-2019		Sturtevant et al (2017-)
US-xUN	University of Notre Dame Environmental Research Center (NEON)	Michigan	46.234	-89.537	Deciduous Broadleaf Forests	Evergreen/mixed forests > 40N	2018-2019		Sturtevant et al (2017-)

Table S3: optimized VPRM parameters for each of the nine PFTs using the original VPRM respiration model with annual and seasonal parameters (i.e. VPRM$_{ann}$ and VPRM$_{seas}$). Deciduous broadleaf forests and urban PFTs share the same parameters, and T$_{min}$, T$_{opt}$ and T$_{max}$ parameters are in units of °C. Cells are highlighted in grey where the optimized relationship between temperature and respiration (α) is negative.

		Deciduous Broadleaf Forest & Urban	Evergreen/ Mixed Forest, >40°N	Evergreen/ Mixed Forest, <40°N	Shrub/ Savannah	Grass/Pasture/ Dev-open	Wetlands	Crops, other	Crops, corn
	T$_{min}$	0	0	0	0	2	0	0	2
	T$_{opt}$	20	20	20	20	18	20	22	25
	T$_{max}$	40	40	40	40	40	40	40	40
	λ	-0.0751	-0.0933	-0.0668	-0.0655	-0.0698	-0.0587	-0.0417	-0.047
	PAR$_0$	745	551	1468	1167	1561	794	2405	11155
	β	1.396	1.094	0.110	0.805	0.879	0.947	0.788	0.925
annual	α	0.099	0.152	0.205	0.072	0.087	0.059	0.076	0.092
	λ	-0.011	-0.1184	-0.0951	-0.0643	-0.1526	-0.1849	-0.114	-0.001
	PAR$_0$	50000	99	882	1134	235	89	273	10
	β	0.983	0.589	0.154	1.224	0.522	0.594	0.380	0.383
winter (DJF)	α	0.024	0.016	0.165	-0.006	0.030	0.034	0.004	0.016
	λ	-0.0678	-0.1052	-0.0759	-0.0635	-0.1066	-0.0792	-0.0844	-0.3065
	PAR$_0$	676	521	1064	1127	900	595	825	61
	β	1.067	0.834	-0.319	-0.244	0.364	0.887	0.231	0.513
sprng (MAM)	α	0.116	0.133	0.238	0.105	0.119	0.044	0.121	0.067
	λ	-0.0847	-0.099	-0.0621	-0.0708	-0.0839	-0.0733	-0.0478	-0.0494
	PAR$_0$	681	549	1647	1061	1158	616	1940	7615
	β	5.650	0.889	12.736	5.875	10.243	6.817	6.460	9.775
summer (JJA)	α	-0.050	0.239	-0.276	-0.095	-0.244	-0.150	-0.133	-0.274
	λ	-0.0901	-0.1309	-0.0848	-0.0754	-0.0978	-0.0746	-0.0414	-0.0433
	PAR$_0$	577	424	955	1059	765	525	1193	3754
	β	1.410	0.617	-0.129	0.756	0.928	0.994	0.662	0.656
fall (SON)	α	0.095	0.226	0.242	0.106	0.093	0.056	0.099	0.119

Table S4: optimized VPRM parameters for each of the nine PFTs using the new respiration model (i.e. VPRM$_{new}$) developed in this study. T_{min}, T_{opt}, T_{max}, and T_{crit} parameters are in units of °C.

	Deciduous Broadleaf Forest & Urban	Evergreen/ Mixed Forest, >40°N	Evergreen/ Mixed Forest, <40°N	Shrub/ Savannah	Grass/Pasture/ Dev-open	Wetlands	Crops, other	Crops, corn
T_{min}	0	0	0	0	2	0	0	2
T_{opt}	20	20	20	20	18	20	22	25
T_{max}	40	40	40	40	40	40	40	40
T_{crit}	11	3	8	11	7	12	7	-1
T_{scale}	0.15	0.05	0.1	0.15	0	0.05	0	0
λ	-0.098	-0.124	-0.081	-0.106	-0.119	-0.096	-0.068	-0.076
PAR_0	585	436	1203	655	850	501	1252	2854
β	-5.357	0.232	0.673	-4.464	-1.580	-7.892	-1.351	-0.123
α_1	0.782	0.073	-0.067	0.685	0.293	1.090	0.246	0.072
α_2	-0.0203	0.0048	0.0107	-0.0184	-0.0091	-0.0331	-0.0062	-0.0013
γ	4.87	3.03	2.38	4.35	4.19	4.68	3.66	5.05
θ_1	2.370	-1.639	-4.744	-0.764	-1.709	1.852	-0.230	0.189
θ_2	-0.365	0.418	0.666	0.057	0.240	-0.439	-0.012	-0.137
θ_3	0.0137	-0.0132	-0.0184	0.0031	0.0010	0.0221	0.0080	0.0155

Table S5: Towers with observed CO_2 mole fraction data calibrated to the WMO-CO2-X2007 scale, sorted from north to south. Also shown are other tower characteristics, months with observations from November 2016 to October 2017, and the percentage of each land cover within the footprint on average for the full year, calculated using the average of WRF-STILT and NAMS-STILT transport. Data providers are National Oceanic and Atmospheric Administration (NOAA), Earth Networks (EN), Environment Canada (EC), Harvard University (HU) and Penn State University (PSU). The data provider 'EN-NIST' refers to towers operated by Earth Networks and funded by the National Institute of Standards & Technology (NIST; Karion et al, 2020). Tower locations are also shown in Figure 2 of the main text.

Name	Description	Data Provider	Latitude	Longitude	Elevation (masl)	Inlet height (m)	Months with data	DBF	ENF/MF, >40N	ENF/MF, <40N	Wetlands	Shrubs	Crops	Grass/ pasture/ dev-open	Developed (low/med/high)
LEF	Park Falls, WI	NOAA	45.945	-90.273	474	396	all	30	18	0	30	1	11	8	1
AMT	Argyle, ME	NOAA	45.035	-68.682	53	107	all	17	45	1	15	3	6	9	4
DNH	Durham, NH	EN-NIST	43.709	-72.154	560	100	all	28	34	1	7	2	9	13	5
UNY	Utica, NY	EN-NIST	42.879	-74.785	489	45	all	31	17	2	8	2	14	21	4
TPD	Turkey Point, Ontario	EC	42.617	-80.550	198	35	all	23	9	2	7	1	37	14	6
HAF	Harvard_Forest	HU	42.538	-72.172	344	29	all	28	31	2	10	2	8	14	7
MSH	Mashpee_MA	EN-NIST	41.657	-70.498	32	46	all	20	28	3	10	2	8	16	14
MLD	Mildred, PA	PSU	41.466	-76.419	591	61	all	36	16	3	6	2	14	18	5
BRI	Bremen, IN	EN-NIST	41.458	-86.194	252	100	Dec-Oct	16	4	2	8	1	50	13	7
HCT	Hamden, CT	EN-NIST	41.434	-72.945	197	100	Nov-Mar, Jul	34	17	3	8	2	10	17	11
SNJ	Stockholm, NJ	EN-NIST	41.144	-74.539	407	53	Nov-May	36	13	3	8	1	12	19	7
S01	Mooresville, IN	PSU	39.581	-86.421	256	121	all	25	2	5	4	1	44	16	5
TMD	Thurmont_MD	EN-NIST	39.577	-77.488	564	113	May-Oct	34	6	9	5	1	17	22	6
BUC	Bucktown_MD	EN-NIST	38.460	-76.043	3	75	all	22	5	12	18	2	21	16	6
SFD	Stafford_VA	EN-NIST	38.446	-77.530	76	152	Jul-Oct	31	5	15	7	2	14	21	6
RIC	Richmond, VA	EN-NIST	37.509	-77.576	89	95	all	27	3	19	7	2	14	21	7
SKY	Somerset, KY	EN-NIST	36.961	-84.568	375	100	Apr-Jul	37	1	14	3	1	15	25	4
DVA	Danville, VA	PSU	36.706	-79.437	278	215	Dec-Oct	33	2	18	4	3	12	24	5
MNC	Middlesex, NC	EN-NIST	35.831	-78.145	73	213	Nov-Mar, May-Oct	20	2	22	13	2	19	18	5
SMT	Signal Mountain, TN	EN-NIST	35.207	-85.286	610	100	Nov-Apr	36	1	16	3	2	11	26	6
SCT	South Carolina Tower	NOAA	33.406	-81.833	114	305	all	16	1	23	20	5	12	18	5

Table S6: Adjusted R^2's from regressions predicting night-time average NEE observations with site-specific meteorological and remote-sensing data for each PFT. Each column includes additional predictor variables into the model, and the last column adds the low air temperature correction to the full model with all variables. Cells are highlighted where the addition of the extra variable(s) in that column increased the adjusted R^2 by >= 0.025 for that PFT.

	T	$T+T^2$	$T+T^2$+EVI	$T+T^2$+EVI+Wscale+Wscale*T+Wscale*T^2	$T+T^2$+EVI+Wscale+Wscale*T+Wscale*T^2 (with T_{low} correction)
Deciduous broadleaf forests	0.270	0.299	0.338	0.338	0.338
Evergreen needleleaf & mixed forests, > 40°N	0.457	0.525	0.547	0.550	0.559
Evergreen needleleaf & mixed forests, < 40°N	0.183	0.199	0.203	0.203	0.205
Grasslands/ pasture	0.289	0.326	0.385	0.401	0.408
Wetlands	0.297	0.338	0.383	0.388	0.395
Shrublands/ savannah	0.173	0.180	0.242	0.305	0.329
Corn	0.348	0.447	0.593	0.618	0.622
Soybean/ other crops	0.279	0.305	0.494	0.531	0.537

Table S7: Seasonal statistics for winter months (DJF) comparing hourly convolutions to observed biologic enhancements at each tower, averaging convolutions from WRF-STILT and NAMS-STILT and with towers sorted from north to south. The best performing biospheric model(s) for each tower, defined as the lowest values for mean bias (MB in µmol/mol) and root mean squared error (RMSE in µmol/mol) and highest values for correlations (r) and Nash-Sutcliffe coefficients (NSC), are shown in grey (within 0.05 for MB and RMSE and 0.01 for r and NSC), with the "best" model in red and bold. None of the metrics are highlighted for a tower/model combination with zero or negative NSC. Averaged metrics across towers are shown in the last two rows (with mean absolute values in 2nd row).

	VPRM$_{ann}$				VPRM$_{seas}$				VPRM$_{new}$				CASA				SiB4			
	MB	RMSE	r	NSC	MB	RMSE	r	NSC	MB	RMSE	r	NSC	MB	RMSE	r	NSC	MB	RMSE	r	NSC
LEF	0.15	2.45	0.38	0.14	0.00	2.45	0.41	0.14	-0.04	2.47	0.37	0.13	0.47	2.73	0.25	-0.06	1.23	3.04	0.24	-0.32
AMT	-0.94	2.91	0.41	0.07	-1.18	2.94	0.48	0.05	-1.09	2.91	0.48	0.07	-0.06	2.88	0.41	0.09	0.61	2.86	0.46	0.10
DNH	-0.49	2.48	0.64	0.38	-0.88	2.76	0.60	0.24	-0.81	2.63	0.67	0.31	0.74	2.63	0.62	0.31	1.77	3.11	0.62	0.03
UNY	-0.31	2.78	0.40	0.09	-0.78	2.84	0.37	0.05	-0.81	2.77	0.41	0.09	0.96	3.13	0.43	-0.16	2.01	3.58	0.45	-0.52
TPD	-0.73	3.22	0.56	0.27	-1.51	3.65	0.48	0.07	-1.33	3.44	0.55	0.17	0.85	3.39	0.58	0.20	1.32	3.73	0.48	0.03
HAF	0.46	3.45	0.46	0.20	-0.02	3.47	0.46	0.19	0.06	3.45	0.47	0.20	1.75	4.10	0.39	-0.12	2.66	4.28	0.51	-0.23
MSH	-0.59	3.04	0.58	0.27	-0.96	3.26	0.56	0.16	-0.87	3.20	0.57	0.19	-0.01	3.03	0.53	0.28	0.76	3.05	0.55	0.26
MLD	-0.58	3.34	0.23	-0.13	-1.28	3.46	0.17	-0.21	-1.04	3.29	0.25	-0.09	0.43	3.65	0.21	-0.34	1.34	3.48	0.34	-0.23
BRI	-1.63	4.35	0.65	0.23	-2.62	5.22	0.65	-0.11	-2.13	4.69	0.71	0.10	-0.37	3.78	0.67	0.42	0.65	4.00	0.61	0.35
HCT	-1.98	6.15	0.48	0.10	-2.55	6.51	0.45	-0.02	-2.42	6.39	0.50	0.02	-1.47	6.15	0.39	0.09	-0.40	6.01	0.37	0.14
SNJ	-0.31	4.93	0.19	-0.03	-1.00	4.96	0.17	-0.04	-0.86	4.86	0.21	0.01	0.45	5.08	0.18	-0.09	1.63	5.12	0.28	-0.11
S01	-1.16	3.43	0.62	0.27	-1.99	4.08	0.49	-0.03	-1.58	3.69	0.62	0.16	-0.20	3.19	0.61	0.37	0.58	3.26	0.60	0.34
TMD	NA	NA	NA	NA	NA	NA	NA	NA	NA	NA	NA	NA	NA	NA	NA	NA	NA	NA	NA	NA
BUC	-0.95	3.01	0.53	0.20	-1.71	3.50	0.42	-0.08	-1.29	3.20	0.53	0.10	0.03	2.89	0.52	0.26	0.34	3.08	0.43	0.16
SFD	NA	NA	NA	NA	NA	NA	NA	NA	NA	NA	NA	NA	NA	NA	NA	NA	NA	NA	NA	NA
RIC	-1.46	4.66	0.51	0.13	-2.22	5.11	0.42	-0.05	-1.85	4.76	0.60	0.09	-0.26	4.47	0.44	0.19	-0.48	4.44	0.48	0.21
SKY	NA	NA	NA	NA	NA	NA	NA	NA	NA	NA	NA	NA	NA	NA	NA	NA	NA	NA	NA	NA
DVA	-1.12	4.84	0.58	0.21	-2.23	5.46	0.66	-0.01	-1.63	5.02	0.66	0.15	-0.12	4.76	0.50	0.23	-0.47	5.06	0.38	0.13
MNC	-0.97	4.74	0.52	0.17	-1.84	5.23	0.38	-0.01	-1.36	4.82	0.57	0.14	0.12	4.74	0.41	0.17	0.07	4.96	0.30	0.09
SMT	-1.89	4.64	0.36	-0.04	-2.70	5.06	0.36	-0.24	-2.34	4.85	0.37	-0.14	-1.21	4.45	0.35	0.04	-1.58	4.56	0.34	-0.01
SCT	-1.08	4.72	0.37	0.08	-1.67	4.96	0.38	-0.02	-1.41	4.78	0.43	0.05	-0.52	4.63	0.35	0.11	-0.90	4.74	0.32	0.07
mean	-0.87	3.84	0.47	0.14	-1.51	4.16	0.44	0.00	-1.27	3.96	0.50	0.10	0.09	3.87	0.44	0.11	0.62	4.02	0.43	0.03
MAE	0.93				1.51				1.27				0.56				1.04			

Table S8: Seasonal statistics for spring months (MAM) comparing hourly convolutions to observed biologic enhancements at each tower. Values are highlighted similarly to Table S7.

	VPRM$_{ann}$				VPRM$_{seas}$				VPRM$_{new}$				CASA				SiB4			
	MB	RMSE	r	NSC	MB	RMSE	r	NSC	MB	RMSE	r	NSC	MB	RMSE	r	NSC	MB	RMSE	r	NSC
LEF	0.62	1.69	0.72	0.44	0.37	1.65	0.71	0.47	0.50	1.67	0.72	0.45	1.07	2.20	0.55	0.05	0.88	1.96	0.63	0.25
AMT	0.82	1.94	0.63	0.27	0.43	1.82	0.63	0.36	0.68	1.84	0.66	0.35	1.32	2.36	0.56	-0.07	0.97	2.15	0.55	0.11
DNH	-0.04	2.10	0.74	0.50	-0.51	2.12	0.75	0.49	-0.16	1.90	0.77	0.59	1.07	2.84	0.54	0.09	0.86	2.43	0.66	0.33
UNY	-0.13	2.59	0.80	0.60	-0.62	2.60	0.80	0.60	-0.27	2.59	0.78	0.60	1.61	3.62	0.63	0.22	1.15	3.04	0.73	0.45
TPD	-0.45	4.35	0.51	0.25	-0.88	4.36	0.54	0.25	-0.44	4.24	0.57	0.29	0.56	4.41	0.51	0.23	-0.31	4.92	0.32	0.05
HAF	0.49	2.42	0.67	0.31	0.02	2.26	0.69	0.40	0.35	2.18	0.70	0.44	1.32	3.15	0.50	-0.16	1.28	2.86	0.60	0.04
MSH	-0.31	3.16	0.17	-0.20	-0.58	3.08	0.19	-0.14	-0.29	2.78	0.32	0.07	0.33	2.99	0.26	-0.07	-0.19	3.37	0.04	-0.36
MLD	-0.16	3.10	0.73	0.52	-0.51	3.04	0.74	0.54	-0.05	2.91	0.77	0.58	0.83	4.09	0.48	0.16	0.18	3.59	0.61	0.36
BRI	-0.19	3.36	0.62	0.37	-0.42	3.43	0.61	0.35	-0.31	3.40	0.62	0.36	0.31	3.27	0.64	0.41	0.43	3.52	0.59	0.31
HCT	-0.25	3.24	0.42	0.17	-0.61	3.28	0.43	0.15	-0.58	3.34	0.40	0.12	0.08	3.25	0.42	0.17	0.41	3.39	0.33	0.09
SNJ	-0.50	3.22	0.64	0.36	-0.80	3.19	0.65	0.37	-0.56	3.07	0.66	0.42	0.38	3.36	0.57	0.31	-0.18	3.66	0.47	0.18
S01	-0.58	4.35	0.51	0.25	-0.59	4.34	0.51	0.25	-0.44	4.07	0.60	0.34	0.20	3.83	0.65	0.42	0.23	4.54	0.43	0.18
TMD	-1.36	4.80	0.31	-0.38	-1.19	4.50	0.32	-0.22	-0.11	4.38	0.33	-0.15	2.42	5.86	0.10	-1.06	0.75	3.62	0.50	0.21
BUC	-0.30	3.85	0.56	0.29	-0.54	3.80	0.58	0.31	0.08	3.48	0.65	0.42	0.93	3.80	0.60	0.31	0.03	4.24	0.40	0.14
SFD	NA	NA	NA	NA	NA	NA	NA	NA	NA	NA	NA	NA	NA	NA	NA	NA	NA	NA	NA	NA
RIC	-0.81	3.90	0.70	0.46	-0.90	3.89	0.70	0.46	-0.35	3.51	0.76	0.56	0.55	3.95	0.67	0.44	-0.55	4.60	0.51	0.25
SKY	-0.76	4.58	0.76	0.56	-0.44	4.64	0.75	0.55	0.31	4.28	0.80	0.62	2.55	5.07	0.77	0.46	1.11	5.92	0.58	0.27
DVA	-1.36	3.83	0.70	0.40	-1.41	3.84	0.69	0.40	-0.85	3.45	0.74	0.51	-0.08	3.63	0.68	0.46	-0.82	4.42	0.48	0.20
MNC	-1.06	4.53	0.59	0.29	-1.15	4.48	0.59	0.30	-0.06	4.11	0.64	0.41	1.06	4.10	0.68	0.41	1.20	4.38	0.65	0.33
SMT	-1.23	4.39	0.33	0.03	-1.38	4.46	0.32	0.00	-1.19	4.16	0.46	0.13	-0.86	4.10	0.45	0.16	-2.57	5.28	0.13	-0.40
SCT	0.19	3.07	0.66	0.43	0.13	3.12	0.65	0.41	0.32	3.11	0.66	0.41	0.04	3.06	0.66	0.43	0.83	3.60	0.59	0.21
mean	-0.37	3.42	0.59	0.30	-0.58	3.39	0.59	0.32	-0.17	3.22	0.63	0.38	0.79	3.65	0.55	0.17	0.28	3.77	0.49	0.16
MAE	0.58				0.67				0.39				0.88				0.75			

Table S9: Seasonal statistics for summer months (JJA) comparing hourly convolutions to observed biologic enhancements at each tower. Values are highlighted similarly to Table S7.

	VPRMann				VPRMseas				VPRMnew				CASA				SiB4			
	MB	RMSE	r	NSC	MB	RMSE	r	NSC	MB	RMSE	r	NSC	MB	RMSE	r	NSC	MB	RMSE	r	NSC
LEF	0.75	3.98	0.47	0.18	1.74	4.35	0.43	0.02	1.32	4.11	0.47	0.13	1.12	4.12	0.47	0.12	1.48	4.27	0.47	0.06
AMT	-2.06	5.73	0.28	-0.40	-0.22	4.85	0.34	0.00	-0.60	4.82	0.37	0.01	0.60	5.35	0.28	-0.22	-0.02	5.11	0.29	-0.11
DNH	-3.94	6.28	0.46	-0.60	-1.75	4.91	0.49	0.02	-2.03	4.62	0.58	0.13	0.06	4.61	0.51	0.14	-1.53	5.89	0.29	-0.41
UNY	-4.29	7.03	0.46	-0.52	-1.41	5.57	0.49	0.04	-1.95	5.34	0.55	0.12	0.15	5.74	0.46	-0.02	-1.80	6.65	0.33	-0.36
TPD	-1.36	5.88	0.54	0.20	1.18	5.97	0.51	0.17	1.05	5.13	0.64	0.39	-0.85	5.69	0.56	0.25	-3.51	8.27	0.32	-0.59
HAF	-2.27	5.87	0.38	-0.19	-0.12	5.33	0.39	0.02	-0.29	4.92	0.47	0.17	0.96	5.25	0.47	0.05	-0.56	6.44	0.18	-0.43
MSH	-2.71	5.69	0.28	-0.59	-1.09	4.88	0.24	-0.17	-1.03	4.43	0.39	0.04	0.07	4.55	0.33	-0.02	-1.16	5.41	0.16	-0.44
MLD	-4.47	6.49	0.52	-0.71	-1.82	5.25	0.49	-0.12	-1.73	4.51	0.60	0.17	-0.13	4.87	0.50	0.04	-2.67	6.49	0.35	-0.71
BRI	-1.38	5.70	0.75	0.50	0.31	5.63	0.73	0.51	0.64	4.98	0.79	0.62	0.92	5.47	0.74	0.54	-1.85	7.15	0.58	0.21
HCT	-2.84	6.89	0.27	-0.21	-1.13	6.25	0.32	0.00	-0.45	5.92	0.35	0.11	2.33	6.69	0.29	-0.14	-1.34	6.85	0.19	-0.20
SNJ	-5.18	9.86	0.58	-3.50	-1.00	7.57	0.47	-1.65	-3.32	7.98	0.51	-1.95	-1.62	7.07	0.20	-1.31	-0.89	6.72	0.43	-1.09
S01	0.40	5.82	0.64	0.39	2.07	6.19	0.63	0.30	3.06	6.39	0.66	0.26	1.62	6.04	0.63	0.34	0.32	6.62	0.55	0.20
TMD	-2.99	6.14	0.41	-0.21	-0.88	5.33	0.44	0.09	-0.04	5.07	0.47	0.18	-0.14	5.47	0.46	0.04	-1.20	5.50	0.39	0.03
BUC	-1.36	5.55	0.46	0.14	0.32	5.58	0.39	0.12	1.51	5.10	0.58	0.27	0.79	5.35	0.50	0.20	0.69	5.66	0.37	0.10
SFD	-3.17	7.08	0.48	0.04	-1.24	6.32	0.51	0.24	0.41	5.79	0.61	0.36	-1.16	5.77	0.62	0.36	-0.43	6.28	0.50	0.25
RIC	-2.20	4.92	0.67	0.31	-0.45	4.66	0.62	0.38	0.81	4.09	0.74	0.52	-0.11	4.96	0.60	0.30	0.18	5.20	0.48	0.23
SKY	-1.32	5.01	0.59	0.29	0.35	4.57	0.64	0.41	1.53	5.07	0.59	0.27	0.99	5.79	0.56	0.05	0.44	5.52	0.44	0.13
DVA	-2.51	5.82	0.52	0.10	-0.75	5.43	0.49	0.22	0.77	5.12	0.57	0.31	-0.07	5.71	0.50	0.14	-0.19	5.45	0.47	0.21
MNC	-0.98	5.53	0.53	0.23	0.28	5.50	0.50	0.24	1.89	5.45	0.59	0.25	0.45	5.40	0.55	0.27	0.08	5.68	0.44	0.19
SMT	NA	NA	NA	NA	NA	NA	NA	NA	NA	NA	NA	NA	NA	NA	NA	NA	NA	NA	NA	NA
SCT	-0.39	4.14	0.57	0.32	0.18	4.03	0.60	0.35	0.73	3.96	0.63	0.38	-0.47	3.95	0.62	0.38	-0.15	4.28	0.53	0.27
mean	-2.21	5.97	0.49	-0.21	-0.27	5.41	0.49	0.06	0.11	5.14	0.56	0.14	0.28	5.39	0.49	0.08	-0.71	5.97	0.39	-0.12
MAE	2.33				0.91				1.26				0.73				1.02			

Table S10: Seasonal statistics for fall months (SON) comparing hourly convolutions to observed biologic enhancements at each tower. Values are highlighted similarly to Table S7.

	VPRMann				VPRMseas				VPRMnew				CASA				SiB4			
	MB	RMSE	r	NSC	MB	RMSE	r	NSC	MB	RMSE	r	NSC	MB	RMSE	r	NSC	MB	RMSE	r	NSC
LEF	0.48	3.67	0.78	0.52	0.57	3.74	0.79	0.50	0.61	3.65	0.80	0.52	-0.77	3.88	0.69	0.46	-0.45	4.32	0.58	0.33
AMT	-1.60	6.46	0.47	0.16	-1.81	6.45	0.49	0.16	-0.90	5.60	0.63	0.37	-1.86	6.35	0.51	0.19	-1.28	6.84	0.31	0.06
DNH	-0.95	3.98	0.75	0.53	-1.20	4.00	0.75	0.53	-0.07	3.65	0.79	0.61	-1.36	4.71	0.66	0.34	-0.99	5.61	0.43	0.07
UNY	-1.31	4.82	0.69	0.39	-1.26	4.74	0.69	0.41	-0.44	4.22	0.73	0.53	-1.97	5.09	0.70	0.32	-1.90	6.70	0.41	-0.17
TPD	0.21	4.47	0.75	0.55	0.59	4.56	0.75	0.53	1.19	4.57	0.78	0.53	0.01	4.61	0.72	0.52	1.02	5.36	0.61	0.35
HAF	1.07	3.80	0.79	0.59	0.80	3.72	0.79	0.61	1.88	4.12	0.80	0.52	0.60	4.54	0.67	0.41	0.69	5.67	0.44	0.09
MSH	-0.30	3.23	0.67	0.45	-0.38	3.22	0.68	0.46	0.18	3.18	0.70	0.47	0.15	3.34	0.64	0.41	0.70	3.75	0.53	0.26
MLD	-0.78	4.59	0.71	0.49	-0.79	4.56	0.71	0.49	0.30	4.38	0.74	0.53	-1.42	5.41	0.60	0.28	-2.34	6.70	0.36	-0.10
BRI	-0.54	4.88	0.80	0.62	0.39	4.88	0.82	0.62	0.44	4.70	0.82	0.65	-1.16	5.65	0.72	0.49	1.96	6.17	0.71	0.39
HCT	NA	NA	NA	NA	NA	NA	NA	NA	NA	NA	NA	NA	NA	NA	NA	NA	NA	NA	NA	NA
SNJ	NA	NA	NA	NA	NA	NA	NA	NA	NA	NA	NA	NA	NA	NA	NA	NA	NA	NA	NA	NA
S01	0.19	3.97	0.78	0.60	0.74	4.09	0.78	0.58	0.99	4.53	0.71	0.48	-0.11	4.69	0.68	0.45	2.78	5.60	0.68	0.21
TMD	-0.64	5.75	0.78	0.54	-0.31	5.82	0.78	0.53	0.86	5.88	0.77	0.52	-0.66	6.88	0.59	0.34	0.60	7.70	0.45	0.18
BUC	0.31	4.05	0.75	0.54	0.65	4.12	0.75	0.53	1.08	4.08	0.78	0.53	0.13	4.59	0.65	0.41	1.47	5.20	0.57	0.24
SFD	0.05	4.23	0.79	0.58	0.24	4.29	0.79	0.56	1.34	4.44	0.79	0.53	-0.10	5.22	0.60	0.36	0.75	5.86	0.48	0.19
RIC	0.28	3.81	0.79	0.60	0.45	3.84	0.79	0.59	1.14	4.02	0.79	0.56	0.29	4.40	0.69	0.47	0.54	5.25	0.51	0.24
SKY	NA	NA	NA	NA	NA	NA	NA	NA	NA	NA	NA	NA	NA	NA	NA	NA	NA	NA	NA	NA
DVA	-0.51	3.91	0.81	0.62	-0.25	3.85	0.82	0.63	0.92	4.00	0.81	0.60	-0.87	4.64	0.69	0.46	0.94	5.57	0.54	0.22
MNC	0.16	3.53	0.78	0.61	0.56	3.59	0.79	0.59	0.98	3.85	0.76	0.53	-0.07	3.96	0.71	0.50	1.93	5.17	0.56	0.16
SMT	NA	NA	NA	NA	NA	NA	NA	NA	NA	NA	NA	NA	NA	NA	NA	NA	NA	NA	NA	NA
SCT	0.43	3.42	0.75	0.50	0.67	3.53	0.75	0.47	1.09	3.89	0.65	0.35	-0.20	3.41	0.71	0.50	1.96	4.78	0.49	0.02
mean	-0.20	4.27	0.74	0.52	-0.02	4.29	0.75	0.52	0.68	4.28	0.76	0.52	-0.55	4.79	0.66	0.41	0.49	5.66	0.51	0.16
MAE	0.58				0.68				0.85				0.69				1.31			

Figure S1: Interannual variability in monthly air temperatures (top row) and precipitation (bottom row) from 2001-2020. (These data were obtained from the NASA Langley Research Center POWER Project funded through the NASA Earth Science Directorate Applied Science Program, available at https://power.larc.nasa.gov/).
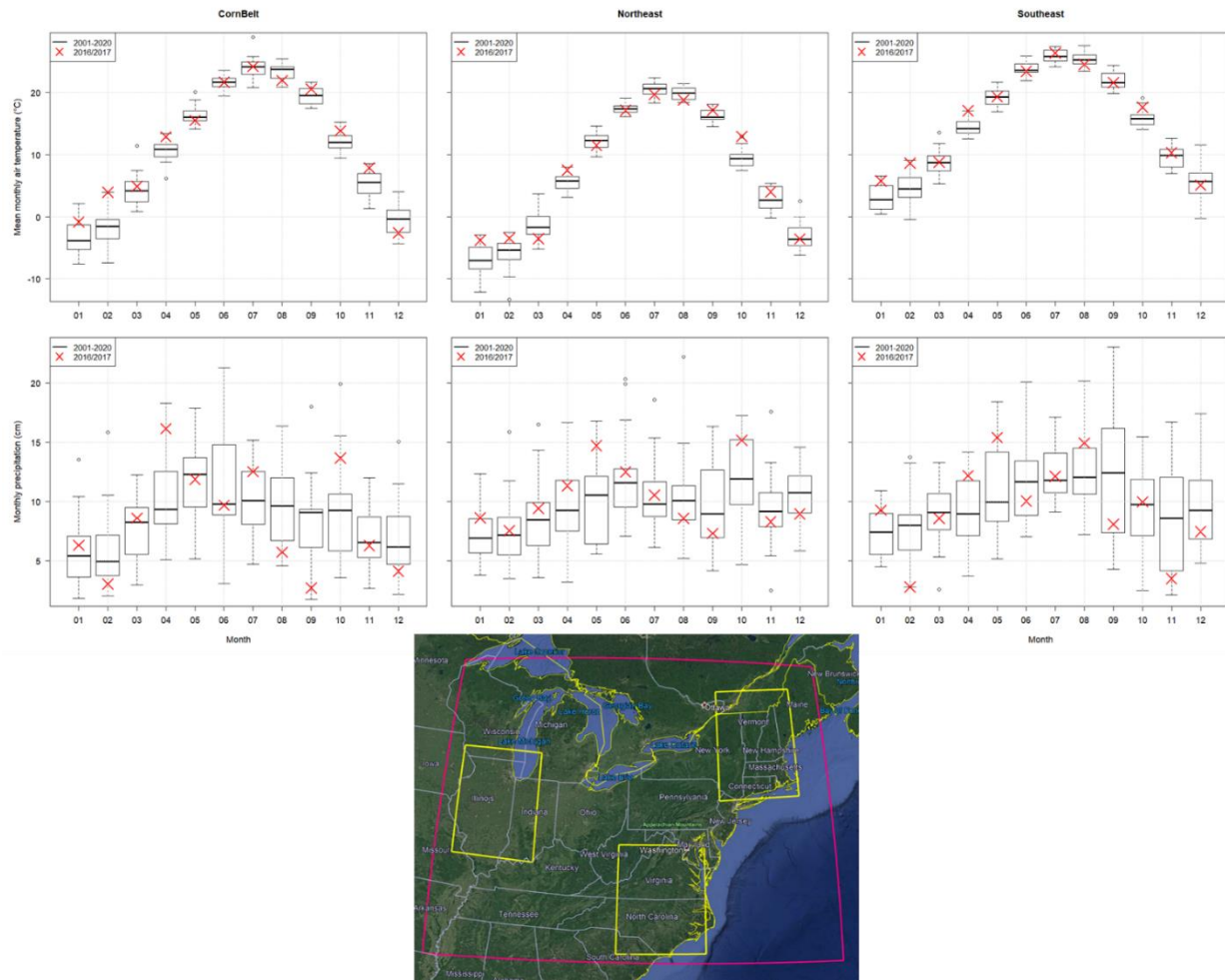
Figure S2: Boxplots of site-specific optimized parameters from the original VPRM model with annual parameters (i.e. VPRM$_{ann}$), clustered by the Plant Functional Type (PFT) classification used in the paper.
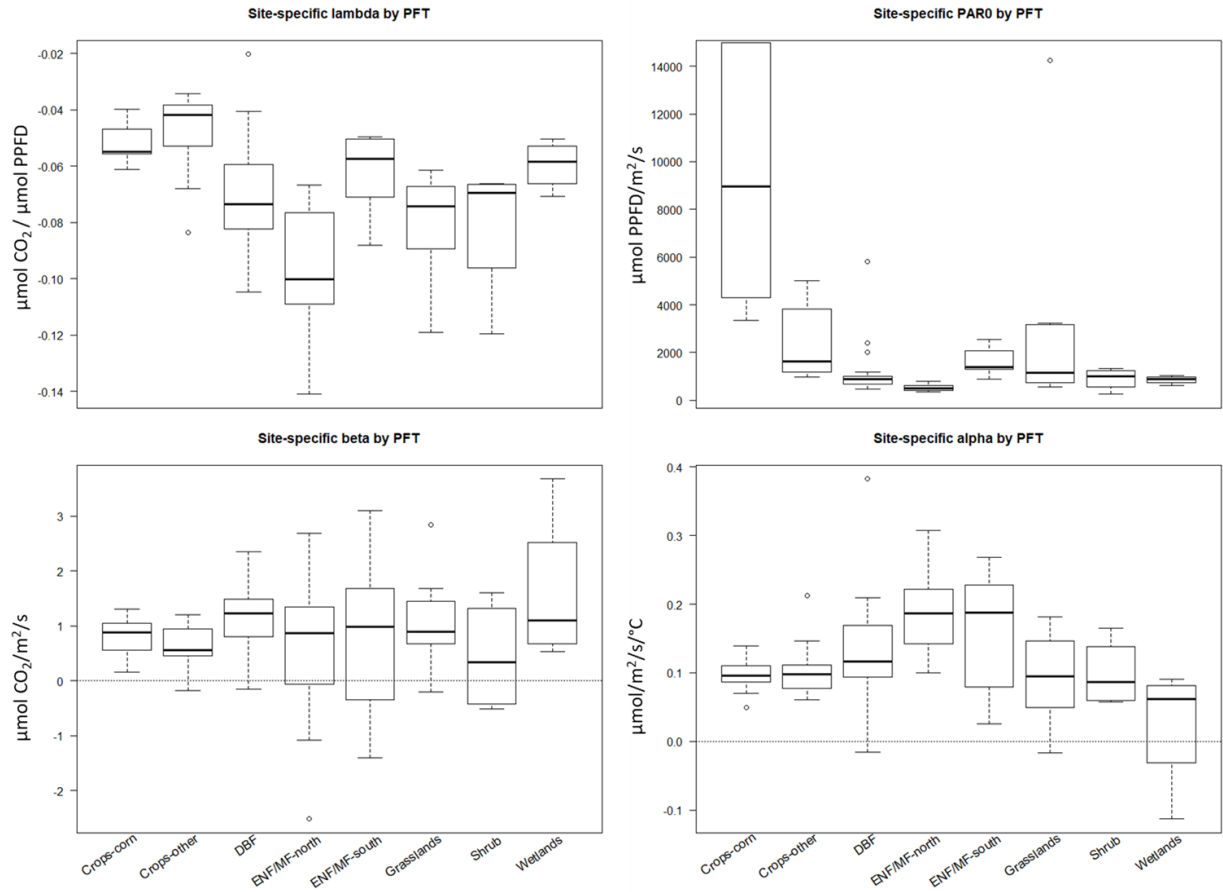
Figure S3: comparison of daily interpolated EVI (from overlapping 16-day MODIS composites) used in VPRM vs. monthly fPAR used in CASA from November 2016 to October 2017. EVI and fPAR data are spatially aggregated across the cropland and deciduous broadleaf forest pixels indicated in Figure 1 of the main text.
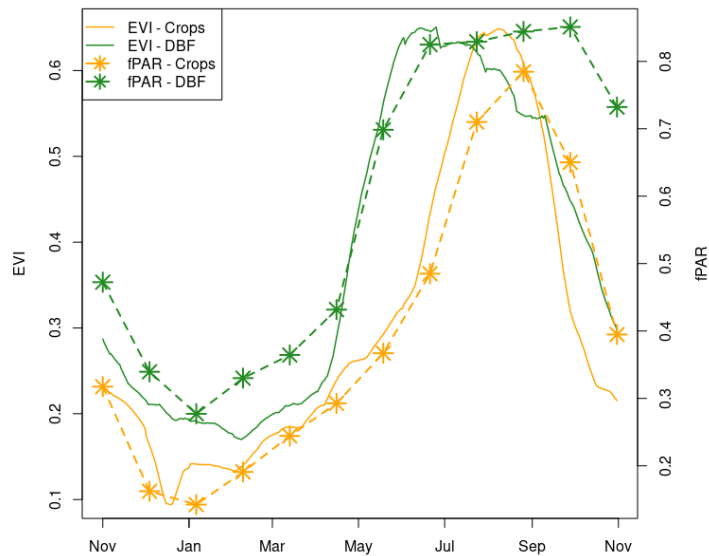
Figure S4: boxplots of monthly mean biases across towers of modeled CO_2 – afternoon average observations for the two versions of Carbon Tracker (2019B and Europe) and their mean. The mean background condition from the two products is used for all months in the atmospheric CO_2 analysis, except July and October, where CT2019B and CTE are used respectively.
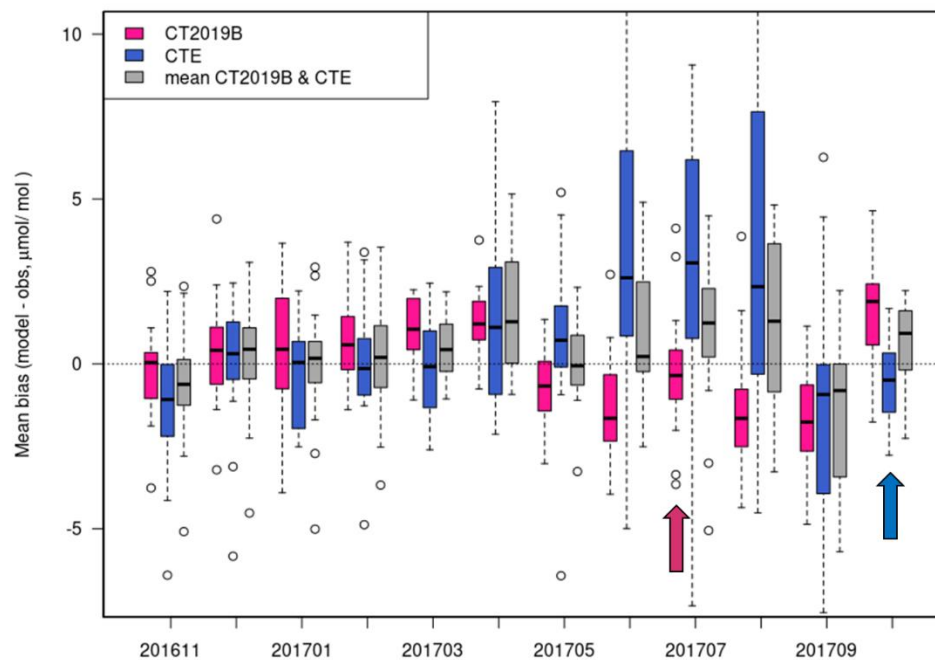
Figure S5: Scatter plots of observed air temperature vs. night-time average NEE for historical flux tower data used in the VPRM parameter optimization. Model fit with $VPRM_{ann}$ is shown in yellow, $VPRM_{seas}$ in light green, and $VPRM_{new}$ in dark green. Also shown are results from a linear regression model fit to just night-time NEE data (purple) for comparison. Results are shown for four PFT's (representing ~36% of total land cover in domain): grasslands (including pasture and developed-open, 17%), evergreen needleleaf/mixed forests <40°N (8%), shrublands and savannah (2%), and wetlands (8%). The NSC values (equivalent to the adjusted r^2 for $VPRM_{new}$ and linear regression model) are also shown to assess relative performance for each model and PFT.
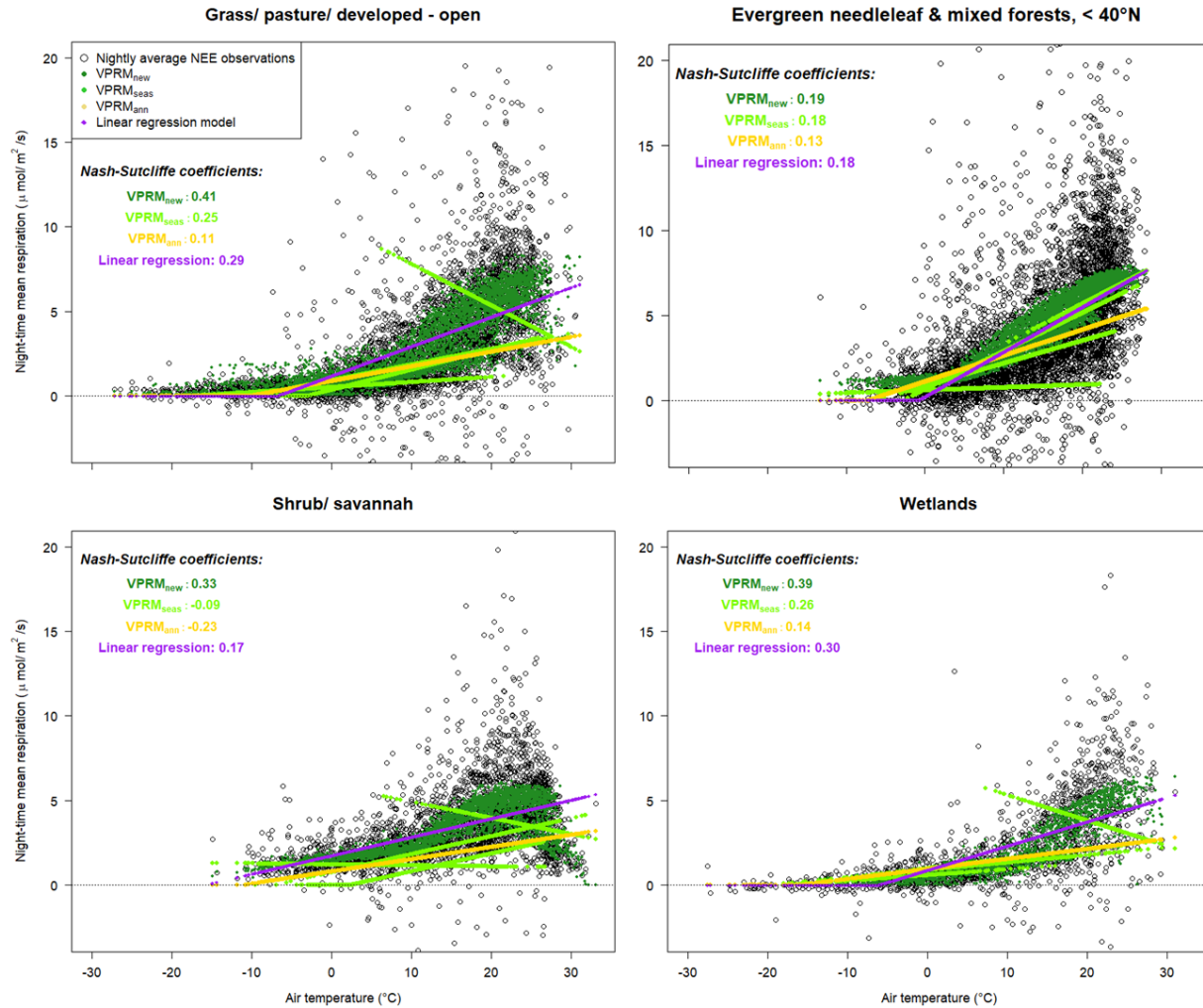
Figure S6: Percent of deciduous broadleaf forests (top row) and croplands (bottom row) at the 0.5°
spatial scale, as seen in the underlying land cover maps for SiB4, VPRM and CASA (with data sources for
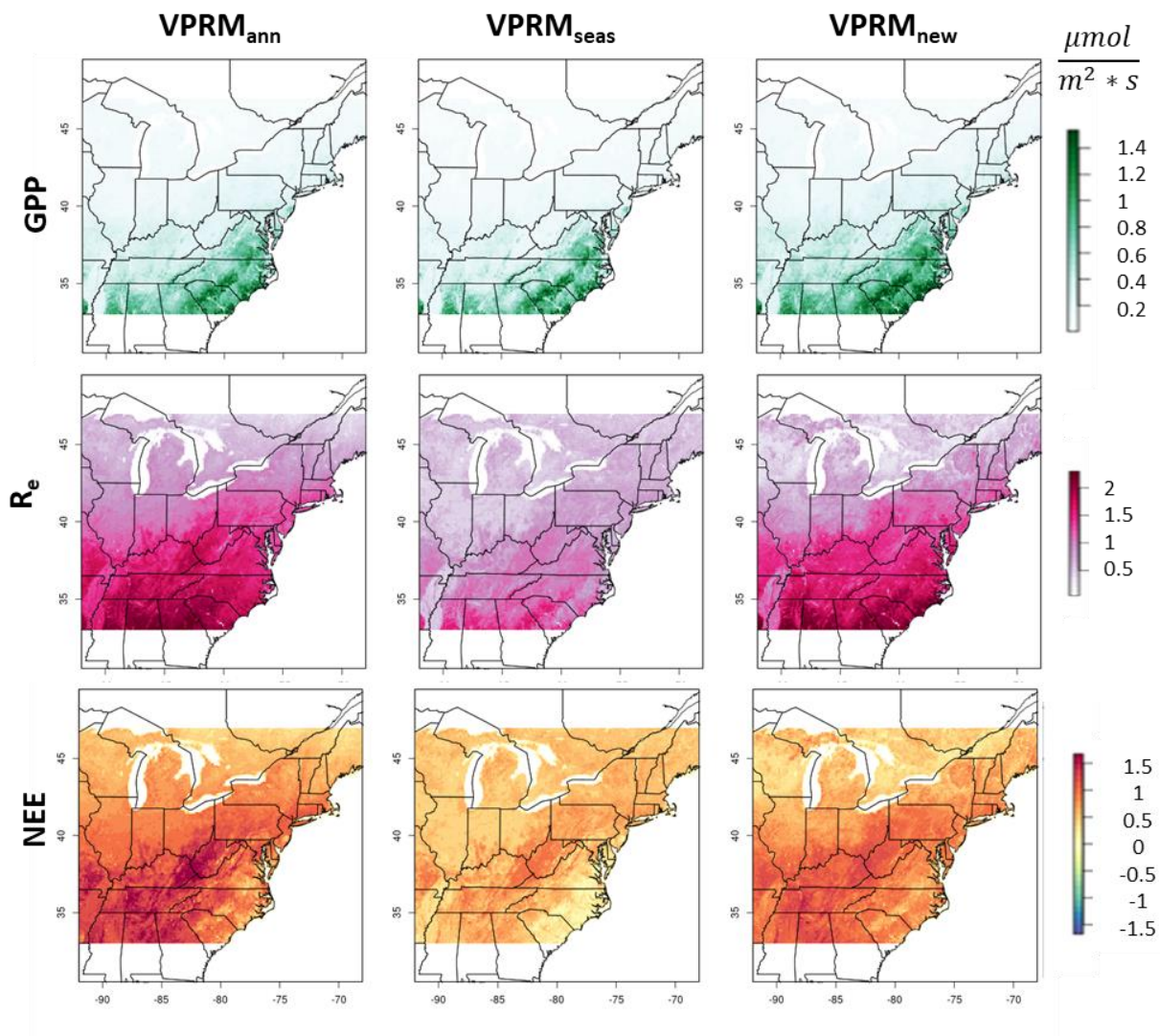each model shown in Table S1). The CASA map is based on the 500 m dominant land cover across the
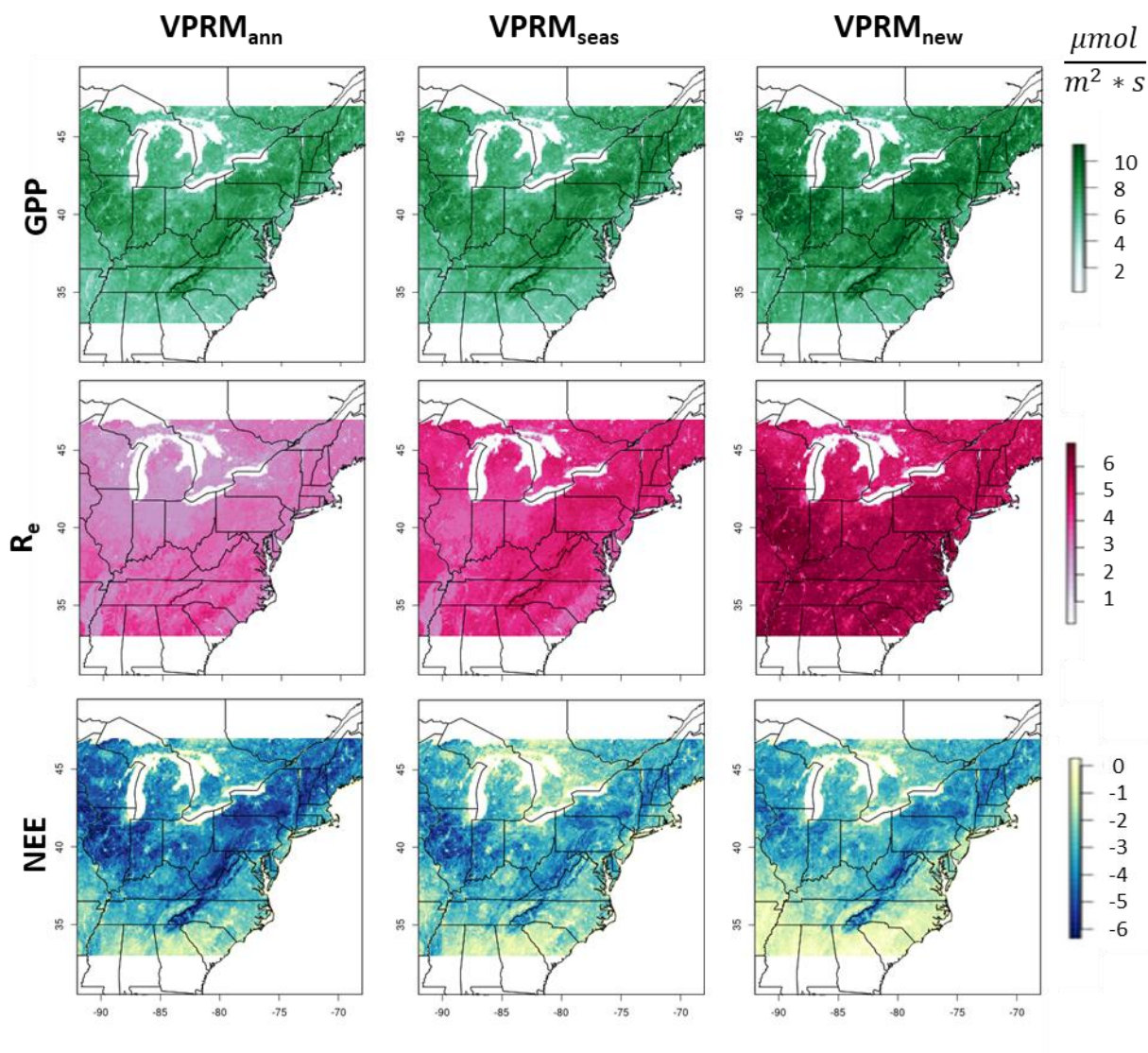domain.
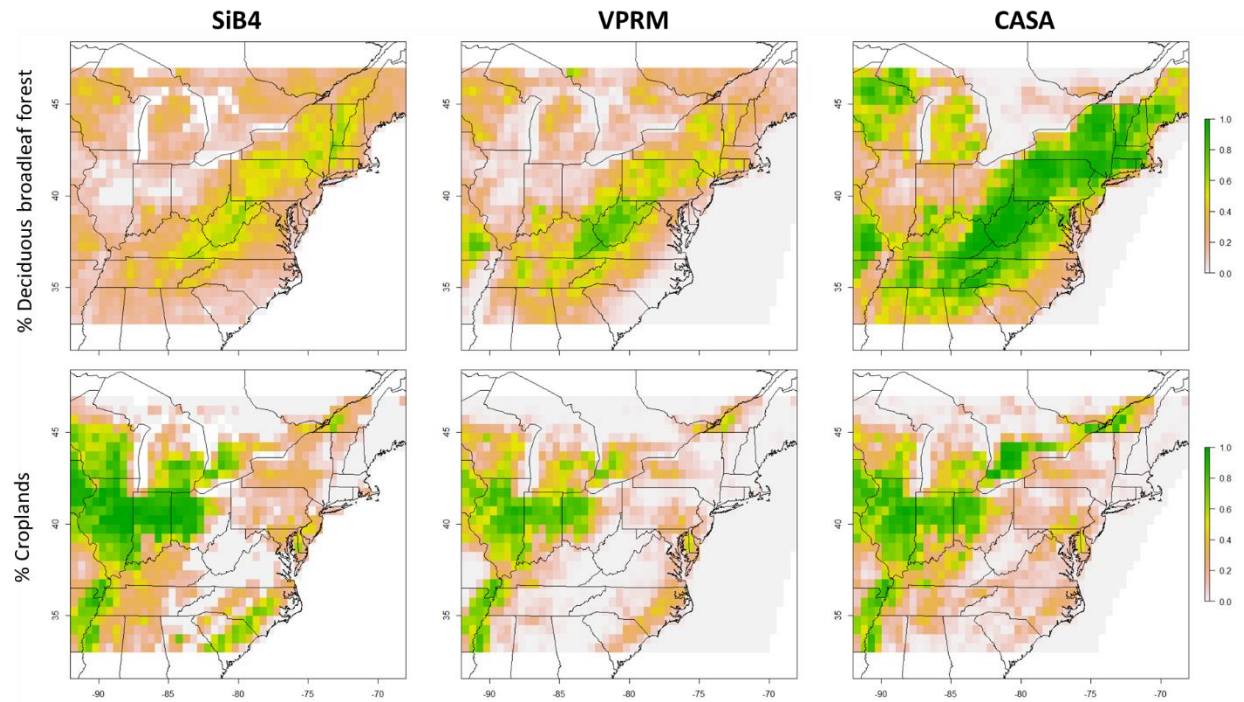
Figure S7: Mean 24-hour gridded GPP, ecosystem respiration (R$_e$) and NEE at 0.1° for the three versions of VPRM (VPRM$_{ann}$, VPRM$_{seas}$, and VPRM$_{new}$) in winter months (December/ January/ February).

Figure S8: Mean 24-hour gridded GPP, ecosystem respiration (R_e) and NEE at 0.1° for the three versions of VPRM (VPRM_ann, VPRM_seas, and VPRM_new) in spring months (March/ April/ May).
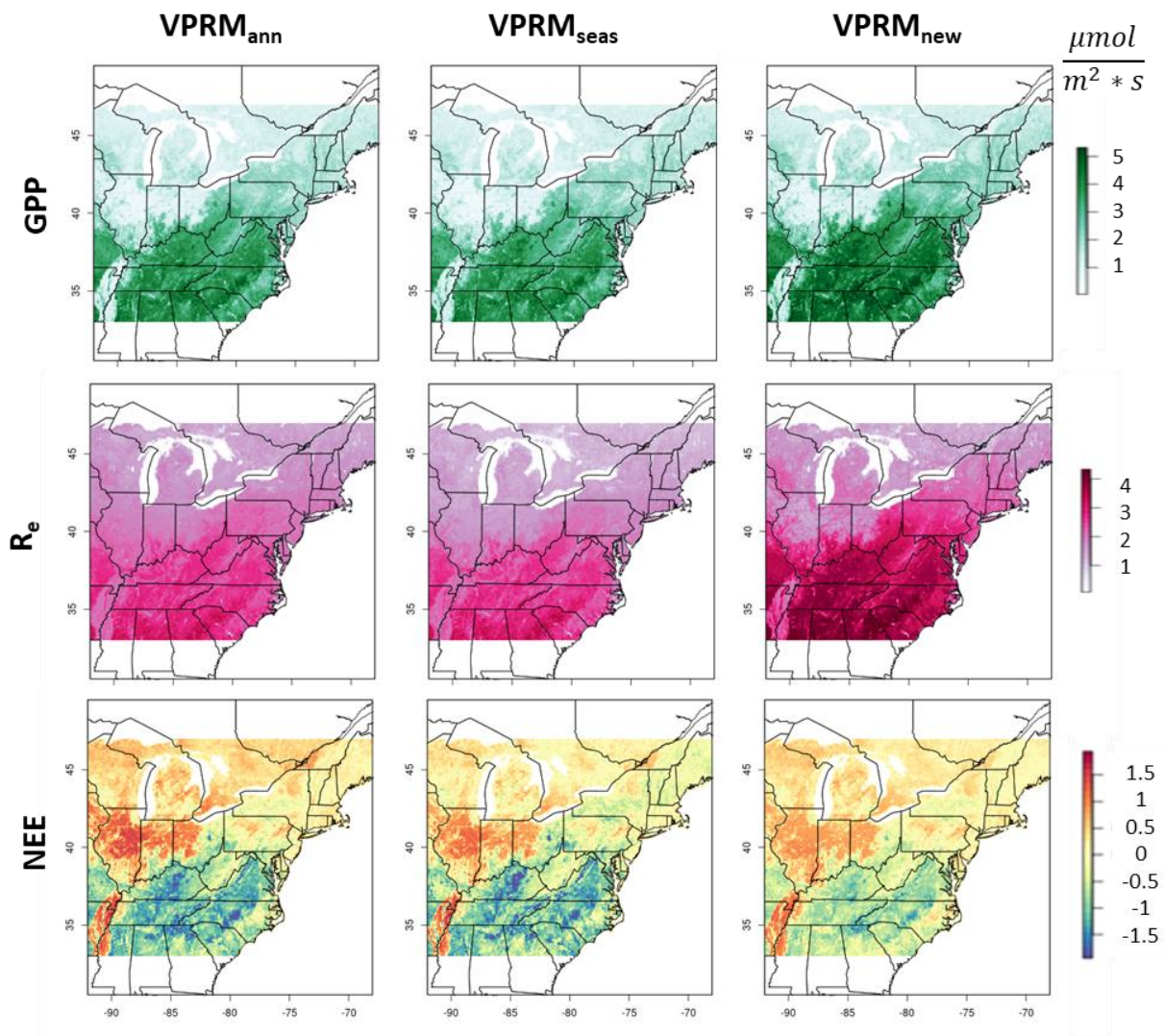
Figure S9: Mean 24-hour gridded GPP, ecosystem respiration (R_e) and NEE at 0.1° for the three versions of VPRM (VPRM$_{ann}$, VPRM$_{seas}$, and VPRM$_{new}$) in summer months (June/ July/ August).

Figure S10: Mean 24-hour gridded GPP, ecosystem respiration (R$_e$) and NEE at 0.1° for the three versions of VPRM (VPRM$_{ann}$, VPRM$_{seas}$, and VPRM$_{new}$) in fall months (September/ October/ November).
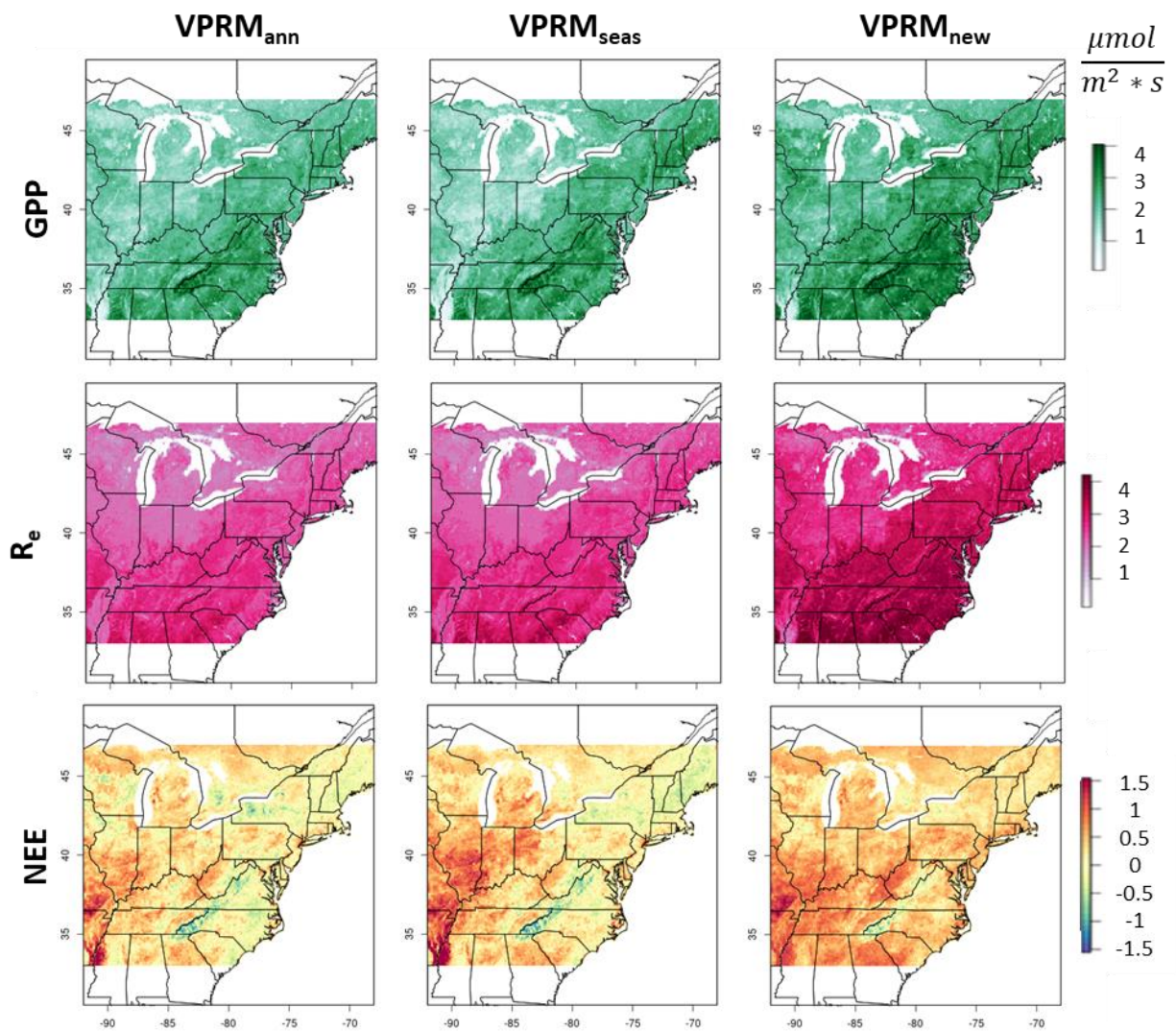
Figure S11: Spatial correlations across different pairs of models (CASA, SiB4, VPRM$_{ann}$, VPRM$_{seas}$, VPRM$_{new}$) for 3-monthly mean gridded GPP, R$_e$ and NEE fluxes.
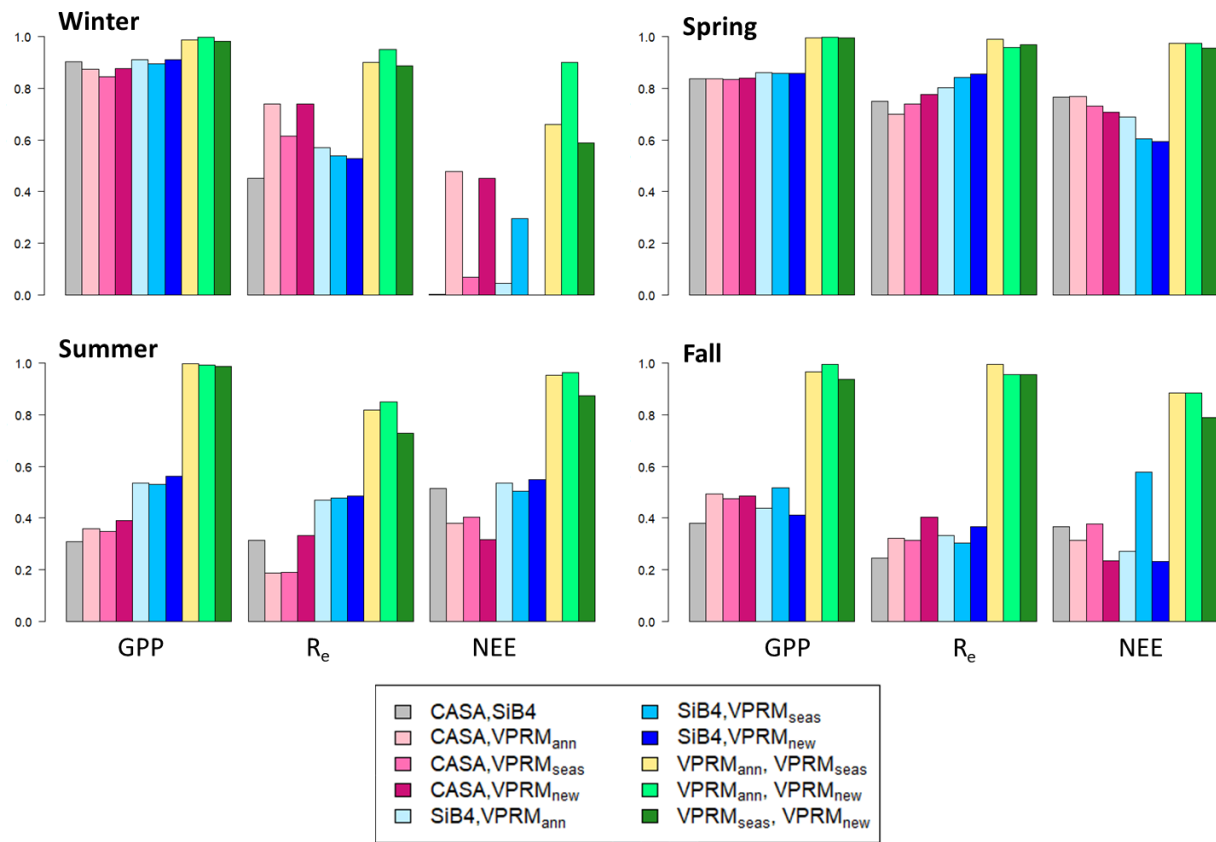
Figure S12: comparison of mean July diurnal cycle of GPP, R_e and NEE for spatially-aggregated deciduous broadleaf forest and cropland pixels (shown in Figure 1 in the main text). Monthly means are shown with dashed lines. All flux units are $\mu mol*m^{-2}*s^{-1}$.
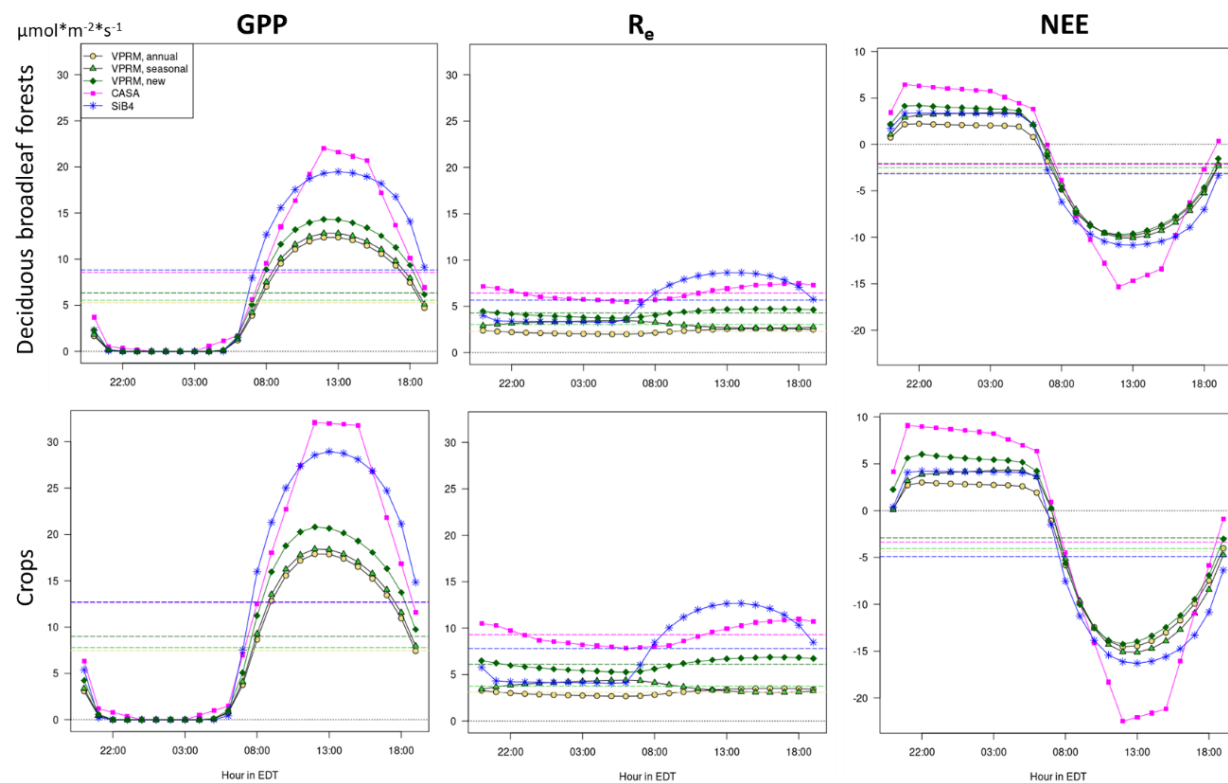
Figure S13: weekly mean observed vs. simulated biological enhancements for VPRM$_{new}$, CASA and SiB4 at the S01 tower in Mooresville, IN using NAMS-STILT transport (left panel) and WRF-STILT transport (right panel). Other details are as described in the caption of Figure 11 in the main text.

	NSC (May-Oct)	R²$_a$ (May-Oct)	NSC (Nov-Apr)	R²$_a$ (Nov-Apr)			NSC (May-Oct)	R²$_a$ (May-Oct)	NSC (Nov-Apr)	R²$_a$ (Nov-Apr)
VPRM$_{new}$	0.62	**0.77**	0.19	0.53		VPRM$_{new}$	0.79	**0.84**	-0.10	0.45
CASA	0.65	0.72	0.45	0.43		CASA	**0.81**	0.80	0.29	0.34
SiB4	**0.66**	0.72	**0.57**	**0.72**		SiB4	0.54	0.70	**0.60**	**0.63**

Figure S14: weekly mean observed vs. simulated biological enhancements for VPRM$_{new}$, CASA and SiB4 at the DNH tower in Durham, NH using NAMS-STILT transport (left panel) and WRF-STILT transport (right panel). Other details are as described in the caption of Figure 11 in the main text.
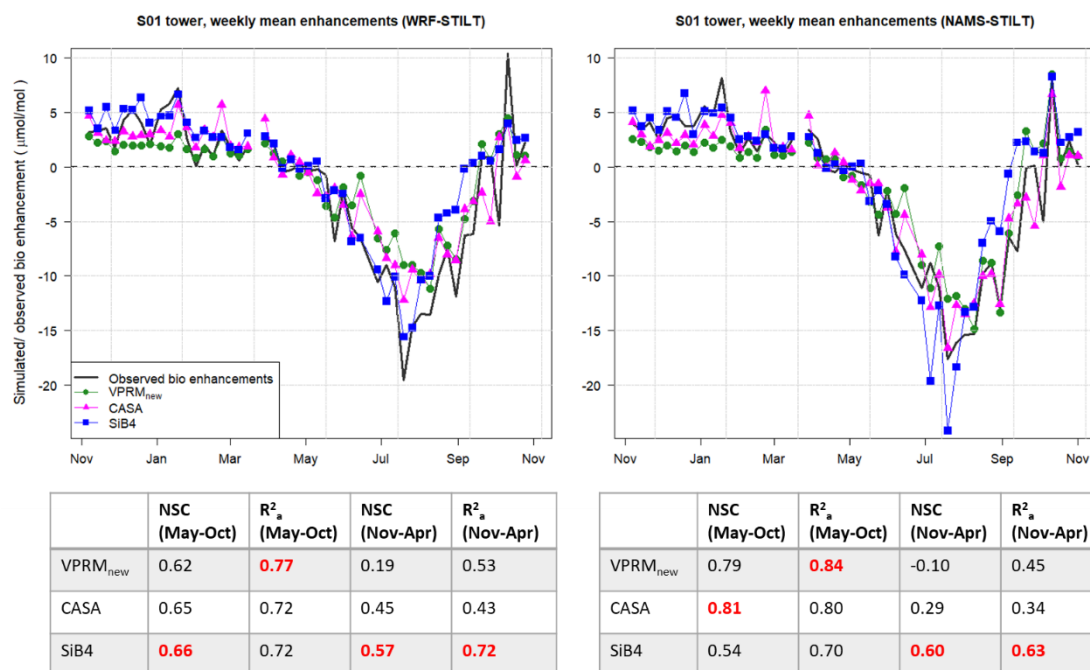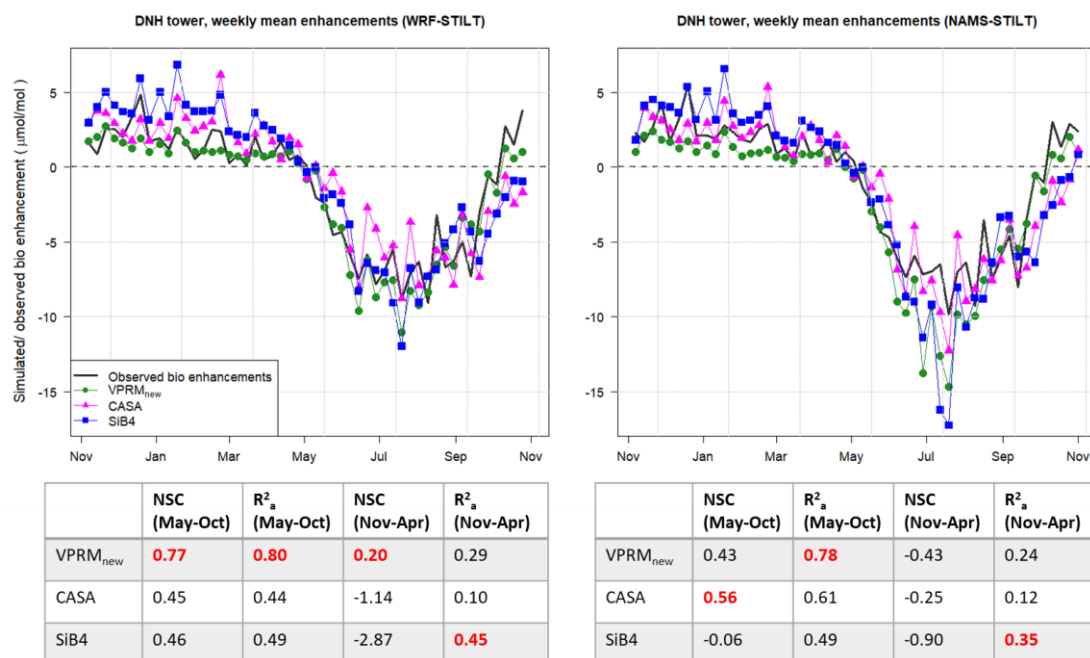

	NSC (May-Oct)	R²$_a$ (May-Oct)	NSC (Nov-Apr)	R²$_a$ (Nov-Apr)			NSC (May-Oct)	R²$_a$ (May-Oct)	NSC (Nov-Apr)	R²$_a$ (Nov-Apr)
VPRM$_{new}$	**0.77**	**0.80**	**0.20**	0.29		VPRM$_{new}$	0.43	**0.78**	-0.43	0.24
CASA	0.45	0.44	-1.14	0.10		CASA	**0.56**	0.61	-0.25	0.12
SiB4	0.46	0.49	-2.87	**0.45**		SiB4	-0.06	0.49	-0.90	**0.35**

Figure S15: Monthly mean biases (simulated - observed) in biospheric CO_2 enhancements from November 2016 to October 2017 across biospheric models using WRF-STILT convolutions (top row) and NAMS-STILT convolutions (bottom row). Also shown are mean absolute errors across towers for both sets of convolutions in the table below. Other details are the same as in Figure 12 in the main text.
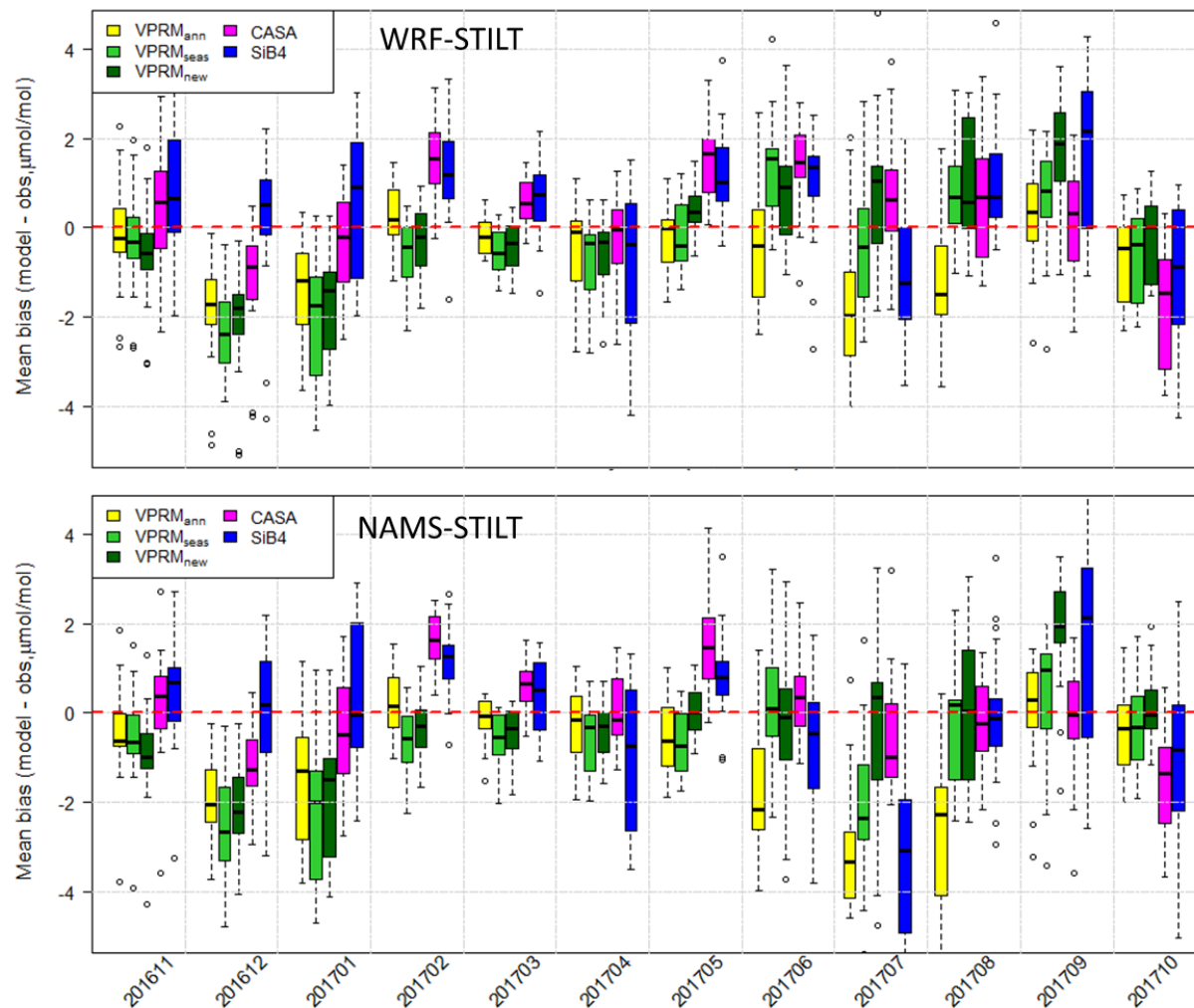
	VPRM_ann	VPRM_seas	VPRM_new	CASA	SiB4
Dec-Feb (WRF)	1.42	1.88	1.65	**1.13**	1.34
Dec-Feb (NAMS)	1.54	2.03	1.79	**1.14**	**1.24**
Mar-May (WRF)	**0.61**	0.74	**0.65**	1.01	1.24
Mar-May (NAMS)	**0.59**	0.72	**0.62**	0.99	1.17
Jun-Aug (WRF)	1.32	**1.10**	**1.06**	1.47	1.48
Jun-Aug (NAMS)	2.30	1.47	**1.10**	**1.17**	2.04
Sep-Nov (WRF)	**1.11**	**1.07**	1.30	1.35	1.60
Sep-Nov (NAMS)	1.49	**1.10**	1.42	**1.16**	1.86

Figure S16: Monthly mean biospheric CO_2 enhancement biases (model – observations) for all towers for each biospheric model (3 versions of VPRM, CASA and SiB4). Mean of WRF-STILT and NAMS-STILT convolutions, Vulcan3.0 fossil fuel emissions and "optimal" background conditions are used for all months. Towers are color-coded to show approximate geographic position and/ or land cover influence (gray: towers near edge of domain, orange: cropland influence, dark green: northeastern US, green: PA/NY/CT, turquoise: mid-Atlantic, blue: southern).
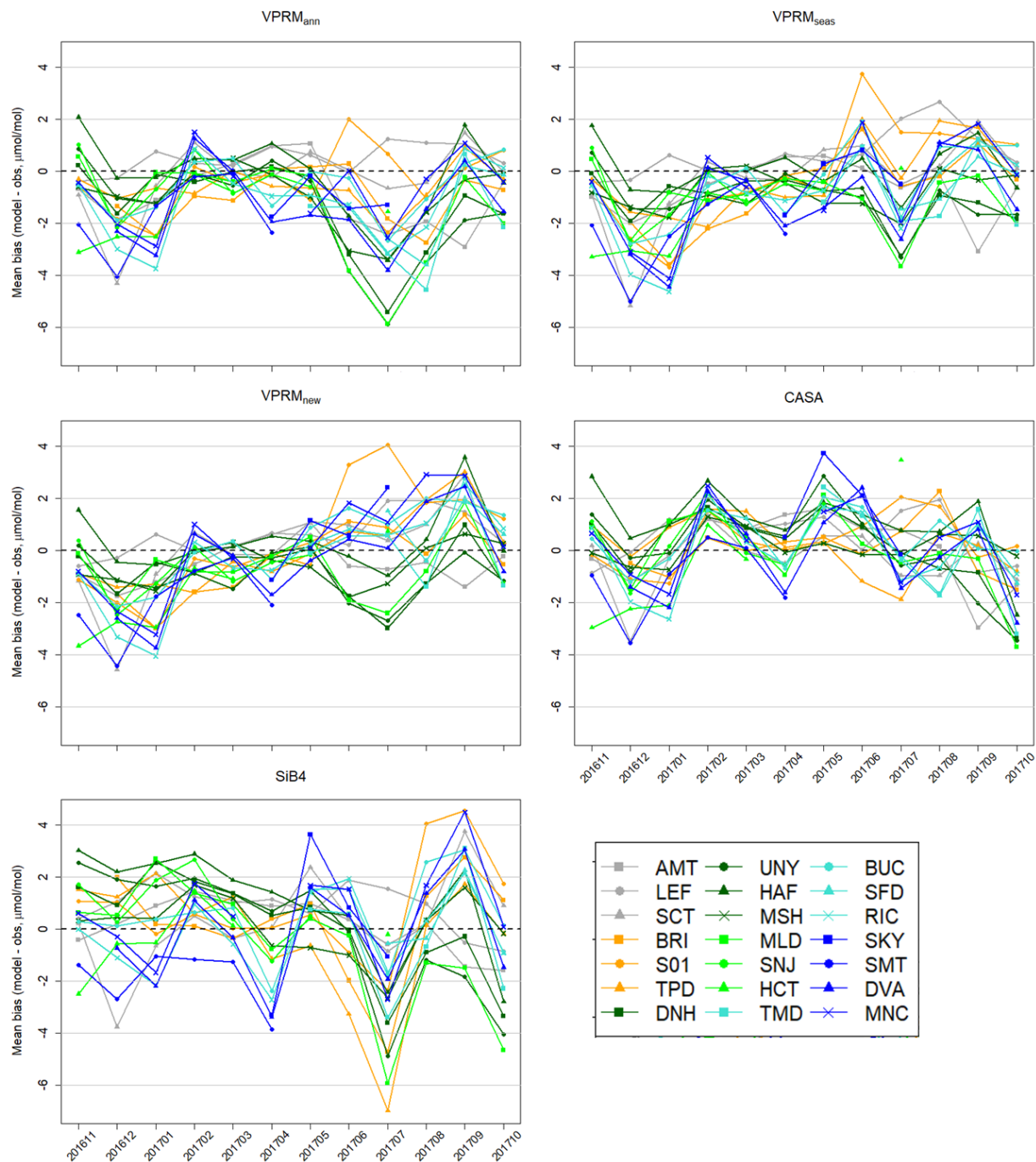
Figure S17: NSC values (top row) and adjusted R^2's (bottom row) for each biospheric model, comparing observed biologic enhancements for each tower against convolved biospheric model. Same as Figure 13 in main text but using WRF-STILT and NAMS-STILT convolutions separately.